

The convergence of discrete period matrices

Felix Günther*

Abstract

We study compact polyhedral surfaces as Riemann surfaces and their discrete counterparts obtained through quadrilateral cellular decompositions and a linear discretization of the Cauchy-Riemann equation. By ensuring uniformly bounded interior and intersection angles of diagonals, we establish the convergence of discrete Dirichlet energies of discrete harmonic differentials with equal black and white periods to the Dirichlet energy of the corresponding continuous harmonic differential with the same periods. This convergence also extends to the discrete period matrix, with a description of the blocks of the complete discrete period matrix in the limit. Moreover, when the quadrilaterals have orthogonal diagonals, we observe convergence of discrete Abelian integrals of the first kind. Adapting the quadrangulations around conical singularities allows us to improve the convergence rate to a linear function of the maximum edge length.

2020 Mathematics Subject Classification: 39A12; 65M60; 30F30.

Keywords: Discrete complex analysis, discrete Riemann surface, discrete Dirichlet energy, discrete period matrix, discrete Abelian integral.

1 Introduction

Over the past few decades, discrete complex analysis has made remarkable progress, even though its development started much later compared to its continuous counterparts. While the continuous theory of complex analysis has a long-established history, its discrete analog emerged relatively recently and is still the subject of ongoing research and exploration.

The concept of discrete harmonicity can be traced back to Kirchhoff's circuit laws, but it was not until almost one hundred years ago that authors such as Coruant, Friedrichs, and Lewy [15] delved into the study of discrete harmonic functions on the square lattice. Subsequently, Isaacs [22] introduced discrete holomorphic functions on the square lattice, with later investigations by Lelong-Ferrand [21, 25] leading to the proof of the Riemann mapping theorem using a limit of discrete holomorphic functions. Expanding the theory, Duffin extended it to rhombic lattices [17, 18], while Mercat [27], Kenyon [23, 24], and Chelkak and Smirnov [13, 14] revived the study of discrete holomorphicity on rhombic lattices from the perspective of statistical physics models such as the Ising model.

Different notions of discrete holomorphicity were explored, including those on triangular lattices by Dynnikov and Novikov [20] and via circle packings and patterns by Stephenson [33], Rodin and Sullivan [30], and Bücking [11]. Bobenko, Mercat, and Suris demonstrated the connection between discrete holomorphic functions and infinitesimal deformations of circle patterns [7], while Bobenko, Pinkall, and Springborn developed a theory of discrete conformally equivalent metrics [8]. Further, Wilson presented a linear theory for discrete complex analysis on triangulated surfaces using holomorphic cochains [35], showing convergence of discrete period matrices to their continuous counterparts.

*Institut für Mathematik, MA 8-3, Technische Universität Berlin, Straße des 17. Juni 136, 10623 Berlin, Germany.
E-mail: fguenth@math.tu-berlin.de.

Mercat’s work on discrete Riemann surfaces and discrete period matrices based on linear discretization [27, 26] laid the groundwork for generalizing the theory to discrete Riemann surfaces composed of general quadrilaterals. Later, Skopenkov’s proof of the uniform convergence of discrete harmonic functions on planar domains decomposed into quadrilaterals with orthogonal diagonals [32], inspired Bobenko and Skopenkov to extend the ideas to discrete Riemann surfaces [9]. They explored discrete harmonic functions on triangulations of polyhedral surfaces and demonstrated convergence of discrete Dirichlet energies, period matrices, and discrete Abelian integrals of the first kind. However, the problem of generalizing the convergence of discrete period matrices to general quadrangulations remained unresolved.

In collaboration with Bobenko, we further developed the linear theory on general bipartite quadrilateral cellular decompositions of Riemann surfaces [5, 6]. Our work, based on the medial graph of the decomposition, established an analogy to the continuous theory, enabling discretizations of linear theorems. In this paper, we continue our exploration by solving the open problem stated by Bobenko and Skopenkov, focusing on the convergence of discrete period matrices on compact polyhedral surfaces. To achieve this, we adapt the approach of Bobenko and Skopenkov and draw inspiration from nonconforming finite element methods developed by Braess [10].

In addition to showing convergence of the discrete period matrix, we specify the limits of the four $g \times g$ -blocks of the complete discrete period matrix, which also considers the discrete holomorphic differentials that do not have equal black and white periods, providing more information on the underlying discrete Riemann surface. Furthermore, for discrete Riemann surfaces decomposed into orthodiagonal quadrilaterals, we demonstrate how the convergence of discrete Abelian integrals of the first kind follows in a manner similar to [9]. Moreover, we present improved error estimates in the convergence proofs, achieving a linear rate in the maximum edge length h by utilizing h -adapted quadrangulations, as defined in [4].

Period matrices play a fundamental role in the study of nonlinear integrable equations [2], making their numerical computation of great interest. Recently, applied algebraic geometry has seen a surge in interest regarding the computation of period matrices. While Riemann surfaces and algebraic curves are equivalent, determining the algebraic curve associated with a Riemann surface is a non-trivial task. This computation involves Riemann theta functions, leading Çelik, Fairchild, and Mandelshtam to coin the term *transcendental divide* for this problem [12]. The period matrix not only determines the Jacobian variety but, according to Torelli’s theorem, also the algebraic curve. Although Deconinck and van Hoesel demonstrated practical methods for computing period matrices of algebraic curves [16], reconstructing the algebraic curve from the period matrix has remained limited to surfaces of low genus, thanks to an algorithm developed by Agostini, Çelik, and Eken [1]. However, the theory of discrete Riemann surfaces offers a valuable tool to approximate the period matrix with known error estimates for compact polyhedral surfaces, which are equivalent to compact Riemann surfaces by a theorem of Troyanov [34].

In Chapter 2, we recapitulate the basic notions of discrete Riemann surfaces as developed in [6], specifically focusing on compact polyhedral surfaces. We then delve into the proof of convergence of the discrete Dirichlet energy in Chapter 3. Building upon this, we demonstrate how the convergence of the discrete Dirichlet energy implies the convergence of the discrete period matrix to the period matrix of the Riemann surface in Chapter 4. Additionally, we address the convergence of discrete Abelian integrals of the first kind in the context of quadrangulations with orthogonal diagonals. Finally, we discuss the application of our convergence results in the paper [12] and outline future research questions in Chapter 5.

2 Discrete Riemann surfaces and their period matrices

In this chapter, we present a concise summary of the linear theory of discrete Riemann surfaces using general quad-graphs. For a more comprehensive understanding and complete proofs, we recommend referring to the detailed explanations in [6]. Our main emphasis is on the discretization of polyhedral surfaces, which can be viewed as both continuous and discrete Riemann surfaces. However, it is important to note that not all discrete Riemann surfaces can be realized as polyhedral surfaces.

In Section 2.1, we begin by clarifying the type of Riemann surfaces we are discretizing. We define discrete Riemann surfaces based on quad-graphs, which serve as our discretization framework. In Section 2.2, we delve into the concept of discrete holomorphicity and define discrete differentials on the medial graph of the quad-graph. The definitions and key properties of discrete period matrices are covered in Section 2.3, where we review their fundamental aspects. Finally, in Section 2.4, we express both the continuous and discrete Dirichlet energy as quadratic forms. These forms involve entries derived from the sums, products, and inverses of the real and imaginary parts of the continuous or the (complete) discrete period matrix.

2.1 Discrete Riemann surfaces

Following the work of Bobenko and Skopenkov [9], we consider the discretization of a *compact polyhedral surface* Σ without boundary. To guarantee the existence of a period matrix, we assume that Σ is not topologically equivalent to a sphere. The surface Σ is constructed by joining Euclidean polygons along shared edges [6]. In other words, Σ possesses a piecewise flat metric, and it exhibits isolated conical singularities [9]. These conical singularities correspond to vertices where the sum of the interior angles of the adjacent polygons deviates from 2π .

Let x and y be two points on the surface Σ . The notation $|xy|$ represents the geodesic distance between these two points. We define the finite set S to be the collection of conical singularities of Σ . Each singularity O in S is associated with an open disk D_O centered at O and has a radius R_O . Importantly, the closure of D_O does not contain any other singularity. The singularity index γ_O is defined as the ratio of $2\pi R_O$ to the circumference of the boundary of D_O . In simpler terms, $2\pi/\gamma_O$ represents the sum of angles at O formed by the polygons incident to this vertex. Geometrically, D_O can be visualized as a cone with an opening angle of $2\pi/\gamma_O$ [9].

The surface Σ possesses a canonical complex structure [3]. To define an atlas, we introduce *polar coordinates* (r, ψ) around each singularity O on the corresponding disk D_O . Here, r ranges from 0 to R_O , and ψ lies in the interval \mathbb{R} modulo $2\pi/\gamma_O$. We define the chart $g_O : D_O \rightarrow \mathbb{C}$ as $g_O(r, \psi) = r^{\gamma_O} \exp(i\gamma_O\psi)$, which corresponds to the complex map $z \mapsto z^{\gamma_O}$.

For points p in Σ excluding the singularities S , we select open disks $D_p \subset \Sigma$ centered at p . These disks do not contain any singularities in their closures. We choose an isometry $g_p : D_p \rightarrow \mathbb{C}$ using the Euclidean metric on \mathbb{C} . If D_p lies completely within a Euclidean polygon of Σ , the choice of g_p is straightforward. If D_p intersects an edge, we flatten D_p along that edge. Different isometries g_p and $g_{p'}$ for p and p' in $\Sigma \setminus S$ are related by an isometry of \mathbb{C} . The transition map $g_O \circ g_p^{-1}$ takes the form $z \mapsto (az + b)^{\gamma_O}$, where a and b are complex numbers with $|a| = 1$. The singularity O is not included in this transition map, specifically excluding $z = -b/a$. Importantly, all transition maps are holomorphic, thus the charts g_x for x in Σ define a complex analytic atlas.

Conversely, it was shown by Troyanov [34] that any compact Riemann surface can be realized as a polyhedral surface.

Definition. A discretization of the Riemann surface Σ , or a *discrete Riemann surface* denoted as (Σ, Λ) , is a finite decomposition Λ of Σ into flat embedded quadrilaterals $F(\Lambda)$. The decomposition satisfies the following properties: The set of conical singularities S is included in the set of vertices $V(\Lambda)$, and the bipartite property holds for the graph $(V(\Lambda), E(\Lambda))$. This decomposition is referred to as a quad-graph, where $V(\Lambda)$, $E(\Lambda)$, and $F(\Lambda)$ represent the sets of vertices, edges, and faces, respectively. The diagonals of the quadrilaterals in $F(\Lambda)$ give rise to two connected graphs called the *black graph* Γ and the *white graph* Γ^* , while \diamond represents the dual graph of Λ . If the diagonals of every quadrilateral in $F(\Lambda)$ intersect each other orthogonally, we call the discretization (Σ, Λ) *orthodiagonal*.

A *discrete chart* $z = z_Q$ of a face Q refers to an isometric embedding of Q into the complex plane \mathbb{C} .

Definition. Given a face $Q \in F(\Lambda)$, its vertices are denoted as b_-, w_-, b_+ , and w_+ in counterclockwise order, with the first vertex being a black vertex. These vertices are identified with their corresponding complex values provided by a discrete chart.

The *discrete complex structure* of (Σ, Λ) is defined by the set of all ρ_Q , where Q ranges over $F(\Lambda)$. The value of ρ_Q is given by

$$\rho_Q = -i \frac{w_+ - w_-}{b_+ - b_-}.$$

In the work presented in [6], it has been shown that a bijective map $z = z_v$ can always be found from the star of a vertex v in Λ to a planar quadrilateral vertex star, preserving the discrete complex structure. This map is also referred to as a *discrete chart*.

It is worth noting that ρ_Q always has a positive real part. In the case where the diagonals b_-b_+ and w_-w_+ are orthogonal to each other, $\rho_Q \in \mathbb{R}^+$. Thus, an orthodiagonal discrete Riemann surface corresponds to a real discrete complex structure.

In their work [9], Bobenko and Skopenkov considered a triangulation Γ with the property that the set of conical singularities S is contained in the set of vertices $V(\Gamma)$. They placed the dual vertices of Γ at the circumcenters of the triangles. When the circumcircles of the triangles do not contain any points other than the three vertices of the triangle, a quad-graph Λ is obtained by connecting the vertices of each triangle in $F(\Gamma)$ with the corresponding dual vertex in $V(\Gamma^*)$. The type of triangulation described above is known as a *Delaunay triangulation*, and the resulting orthodiagonal quad-graph Λ is referred to as the *Delaunay-Voronoi quadrangulation*.

In our research, we expand upon the convergence results presented in [9] by considering general quad-graphs, specifically in relation to period matrices. Additionally, we extend the analysis to encompass general orthodiagonal quad-graphs that may not be derived from a Delaunay triangulation. It is worth noting that the framework established by Bobenko and Skopenkov accommodates scenarios where certain quadrilaterals, denoted by Q , degenerate into lines (indicated by $\rho_Q = 0$) or exhibit negative orientation (indicated by $\rho_Q < 0$). These cases arise when the sum of the two angles opposite an edge is equal to or greater than π , respectively.

It is important to emphasize that while any discrete complex structure with real ρ_Q on a quad-graph Λ can be realized through the discretization process outlined earlier for the Riemann surface Σ , this is not generally applicable when not all ρ_Q are real [6].

2.2 Discrete holomorphicity and discrete differentials

The concept of discrete holomorphicity on quad-graphs is primarily attributed to Mercat [27, 28, 29].

Definition. We define a function $f : V(\Lambda) \rightarrow \mathbb{C}$ to be *discrete holomorphic* if it satisfies the equation

$$f(w_+) - f(w_-) = i\rho_Q(f(b_+) - f(b_-))$$

for all quadrilaterals $Q \in F(\Lambda)$ with vertices b_-, w_-, b_+, w_+ listed in counterclockwise order, starting with a black vertex.

To establish a discrete analogue of exterior calculus, analogous to the continuous setting, the medial graph plays a significant role as the underlying structure for discrete differentials [6]. In Figure 1, the gray-colored vertices represent the medial graph.

Definition. The *medial graph* X of Λ is defined as follows: The vertices of X correspond to the midpoints of the edges in Λ , and an edge $[Q, v]$ connects the midpoints of two edges that share a vertex $v \in V(\Lambda)$ and belong to the same quadrilateral $Q \in F(\Lambda)$. The faces of X , denoted by $F(X)$, are in bijection with $V(\Lambda) \cup F(\Lambda)$.

Each face $F \in F(X)$ associated with a quadrilateral $Q \in F(\Lambda)$ forms a parallelogram when Q is embedded in the complex plane. The edges of F are parallel to the black and white diagonals of Q .

Now, we proceed with the definitions of discrete differentials and discrete two-forms:

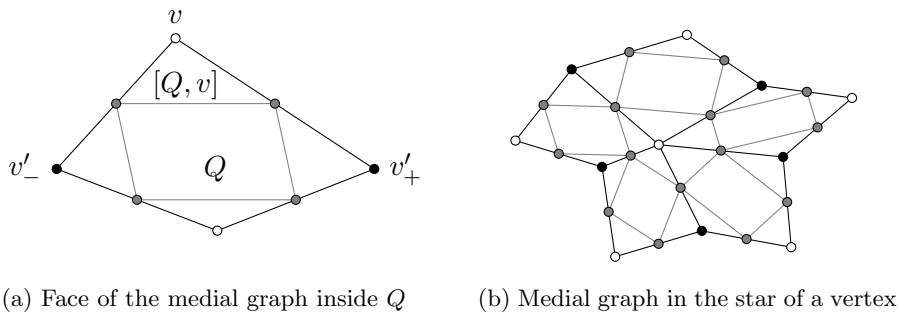


Figure 1: Medial graph X and notation of its edges.

A *discrete differential* ω is a complex-valued function defined on the oriented edges of X . It satisfies the property that $\omega(-e) = \omega(e)$ for differently oriented edges $\pm e$. The evaluation of ω along directed paths or cycles on X is denoted as $\int_P \omega$ and $\oint_P \omega$, respectively. Furthermore, a discrete differential ω is said to be of *type* \diamond if, for every quadrilateral $Q \in F(\Lambda)$, the values of ω on the parallel edges of the corresponding face $F_Q \in F(X)$ are the same. Discrete differentials of type \diamond play a significant role as they are primarily defined on the oriented edges of the quad-graph Λ and its dual graph.

A *discrete two-form* Ω is a complex-valued function defined on the faces of X . The evaluation of Ω on a set of faces is denoted as $\iint_S \Omega$.

The medial graph approach not only allows us to define a natural product between functions defined on either $V(\Lambda)$ or $F(\Lambda)$ and discrete two-forms with matching support, but also enables the definition of a natural product between functions and discrete one-forms. Specifically, the value of a function at a vertex v or a face Q is multiplied by the value of the discrete one-form on all edges $[Q, v]$.

In a chart z associated with a quadrilateral $Q \in F(\Lambda)$ or the star of a vertex $v \in V(\Lambda)$, we can canonically define dz and $d\bar{z}$. These differentials are of type \diamond . Any discrete differential of type \diamond can be locally represented as $pdz + qd\bar{z}$, where p and q are complex functions on $F(\Lambda)$ that depend on the chosen chart.

To define the wedge product $dz \wedge d\bar{z}$ in a chart $z = z_Q$, we set $\iint_{F_Q} dz \wedge d\bar{z} = -4i \text{area}(z(Q))$. Similarly, in a chart $z = z_v$, we define $dz \wedge d\bar{z}$ by $\iint_{F_v} dz \wedge d\bar{z} = -4i \text{area}(z(F_v))$, while $\iint_{F_Q} dz \wedge d\bar{z} = 0$ for faces Q incident to v . The additional factor of 2 compared to the continuous setting accounts for the fact that the parallelograms in the medial graph cover exactly half of the surface area.

Definition. Let $f : V(\Lambda) \rightarrow \mathbb{C}$ and $h : F(\Lambda) \rightarrow \mathbb{C}$. Consider the discrete charts z_Q and z_v associated with $Q \in F(\Lambda)$ and $v \in V(\Lambda)$, respectively, and let F_Q and F_v denote the corresponding faces of X with counterclockwise orientations of their boundaries. We define the *discrete derivatives* $\partial_\Lambda f$, $\bar{\partial}_\Lambda f$, $\partial_\diamond h$, and $\bar{\partial}_\diamond h$ as follows:

$$\begin{aligned} \partial_\Lambda f(Q) &:= \frac{1}{\iint_{F_Q} dz_Q \wedge d\bar{z}_Q} \oint_{\partial F_Q} f d\bar{z}_Q, & \bar{\partial}_\Lambda f(Q) &:= \frac{-1}{\iint_{F_Q} dz_Q \wedge d\bar{z}_Q} \oint_{\partial F_Q} f dz_Q, \\ \partial_\diamond h(v) &:= \frac{1}{\iint_{F_v} dz_v \wedge d\bar{z}_v} \oint_{\partial F_v} h d\bar{z}_v, & \bar{\partial}_\diamond h(v) &:= \frac{-1}{\iint_{F_v} dz_v \wedge d\bar{z}_v} \oint_{\partial F_v} h dz_v. \end{aligned}$$

In the continuous setting, the formulas provided above serve as first-order approximations of derivatives [13]. In the discrete context, a function $f : V(\Lambda) \rightarrow \mathbb{C}$ is discrete holomorphic if and only if $\bar{\partial}_\Lambda f \equiv 0$ in any chart. However, the equation $\bar{\partial}_\diamond h = 0$ is typically dependent on the chosen chart, making the notion of discrete holomorphicity for functions $h : F(\Lambda) \rightarrow \mathbb{C}$ not well-defined on general Riemann surfaces.

The introduced concepts of discrete derivatives for functions, discrete one-forms dz , $d\bar{z}$, and the discrete two-form $dz \wedge d\bar{z}$ allow us to directly adapt the continuous formulas of the exterior derivative, wedge product, Hodge star, scalar product, formal adjoint $\delta := -\star d\star$, Laplacian, harmonicity of functions and one-forms, and holomorphicity of one-forms to the discrete setting.

For instance, the discrete exterior derivative df of a complex function $f : V(\Lambda) \rightarrow \mathbb{C}$ is given locally by $df = \partial_\Lambda f dz + \bar{\partial}_\Lambda f d\bar{z}$. In the case of the discrete wedge product and discrete Hodge star, we need to consider discrete one-forms of type \diamond . The proof of the chart-independence of the discrete formulas corresponds to the previous definitions by Mercat in [27, 29]. For example, the chart-independence of the discrete exterior derivative corresponds to the *discrete Stokes' theorem* $\iint_F d\omega = \oint_{\partial F} \omega$.

2.3 Periods and discrete period matrices

We consider a canonical homology basis $a_1, \dots, a_g, b_1, \dots, b_g$ of $H_1(\Sigma, \mathbb{Z})$. Let $\alpha_1, \dots, \alpha_g, \beta_1, \dots, \beta_g$ be closed paths on X that correspond to the homologies $a_1, \dots, a_g, b_1, \dots, b_g$, respectively. These paths share a common base point $x_0 \in V(X)$, which is fixed throughout the discussion.

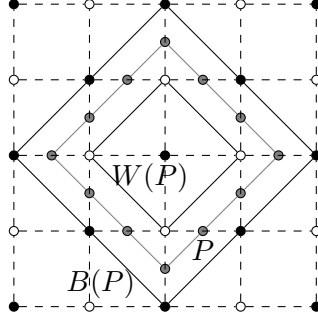


Figure 2: Cycles P on X , $B(P)$ on Γ , and $W(P)$ on Γ^* .

Figure 2 illustrates how each oriented cycle P on X induces closed paths $B(P)$ and $W(P)$ on Γ and Γ^* , respectively, by adding the respective parallel diagonal. We denote the sets of oriented edges of X that are parallel to the edges of $B(P)$ and $W(P)$ as BP and WP , respectively.

Definition. Let ω be a closed discrete differential of type \diamond . For $1 \leq k \leq g$, we define its a_k -periods as $A_k := \oint_{\alpha_k} \omega$ and b_k -periods as $B_k := \oint_{\beta_k} \omega$. We also define its black a_k -periods as $A_k^B := 2 \int_{B\alpha_k} \omega$ and its black b_k -periods as $B_k^B := 2 \int_{B\beta_k} \omega$. Similarly, we define its white a_k -periods as $A_k^W := 2 \int_{W\alpha_k} \omega$ and its white b_k -periods as $B_k^W := 2 \int_{W\beta_k} \omega$.

Clearly, $2A_k = A_k^B + A_k^W$ and $2B_k = B_k^B + B_k^W$. In some cases, it is more convenient to work with the integrals of closed discrete differentials instead. These integrals have a one-to-one correspondence with the discrete differentials and exhibit multi-valued behavior with periods, unless the differential vanishes. We denote the universal cover of (Σ, Λ) as $(\tilde{\Sigma}, \tilde{\Lambda})$, which is a non-compact discrete Riemann surface. The deck transformation corresponding to the closed cycle P on Σ is denoted as d_P .

Definition. A function $f : V(\tilde{\Lambda}) \rightarrow \mathbb{C}$ is said to be *multi-valued* with black periods $A_1^B, A_2^B, \dots, A_g^B, B_1^B, B_2^B, \dots, B_g^B \in \mathbb{C}$ and white periods $A_1^W, A_2^W, \dots, A_g^W, B_1^W, B_2^W, \dots, B_g^W \in \mathbb{C}$ if it satisfies the following conditions:

$$f(d_{\alpha_k} b) = f(b) + A_k^B, \quad f(d_{\alpha_k} w) = f(w) + A_k^W, \quad f(d_{\beta_k} b) = f(b) + B_k^B, \quad f(d_{\beta_k} w) = f(w) + B_k^W$$

for any $1 \leq k \leq g$, each black vertex $b \in V(\tilde{\Gamma})$, and each white vertex $w \in V(\tilde{\Gamma}^*)$.

The periods of closed discrete differentials satisfy a discrete analogue of the classical Riemann bilinear identity. Additionally, for any given set of discrete periods, there exists a unique discrete harmonic differential with these periods. We provide a proof of this theorem in [6], slightly modified below.

Theorem 2.1. *Let $A_k^B, B_k^B, A_k^W, B_k^W, 1 \leq k \leq g$, be $4g$ given complex numbers. Then, there exists a unique discrete harmonic differential ω with these black and white periods.*

Proof. We will prove the statement for real periods. Consider the vector space R of all multi-valued functions $f : V(\tilde{\Lambda}) \rightarrow \mathbb{R}$ that have the given black and white periods. For any such function f , df is a discrete differential of type \diamond on (Σ, Λ) . The discrete Dirichlet energy $E_\diamond(f) := \langle df, df \rangle$ is convex, quadratic, and nonnegative [6], which implies the existence of a minimum $M_0 : V(\tilde{\Lambda}) \rightarrow \mathbb{R}$.

Any element $f \in R$ can be written as $f = M_0 + f'$, where $f' : V(\Lambda) \rightarrow \mathbb{R}$. For $\lambda \in \mathbb{R}$, we have

$$E_\diamond(f) = E_\diamond(M_0) + 2\lambda \langle dM_0, df' \rangle + \lambda^2 E_\diamond(f').$$

Since M_0 is the minimizer, it follows that $\langle dM_0, df' \rangle = 0$ for all functions $f' : V(\Lambda) \rightarrow \mathbb{R}$.

Let $\omega := df$. The discrete differential ω is of type \diamond and has the required periods. Since δ is the formal adjoint of d , we have

$$0 = \langle \omega, df' \rangle = \langle \delta\omega, f' \rangle = \langle \delta dM_0, f' \rangle = -\langle \Delta M_0, f' \rangle,$$

where ΔM_0 is well-defined on (Σ, Λ) . Therefore, we have $\delta\omega = 0 = d\omega$ and $\Delta M_0 = 0$, indicating that M_0 and ω are discrete harmonic. The uniqueness of ω follows from discrete Liouville's Theorem. \square

Corollary 2.2. *If ω is a discrete harmonic differential, then it has the minimal discrete Dirichlet energy $\langle \omega, \omega \rangle$ among all discrete one-forms with the same black and white periods. Furthermore, $\langle \omega, df \rangle = 0$ for all $f : V(\Lambda) \rightarrow \mathbb{C}$.*

An immediate consequence of Theorem 2.1 is that the complex vector space of discrete holomorphic differentials has dimension $2g$. Discrete periods behave similarly to their continuous counterparts, and the bipartiteness of Λ leads to the splitting into black and white periods. This implies the following:

Theorem 2.3. *For any $2g$ complex numbers A_k^B, A_k^W , $1 \leq k \leq g$, there exists exactly one discrete holomorphic differential ω with these black and white a -periods.*

For any $4g$ real numbers $Re(A_k^B), Re(B_k^B), Re(A_k^W), Re(B_k^W)$, there exists exactly one discrete holomorphic differential ω such that its black and white periods have these real parts.

Definition. Let ω_k^B , $1 \leq k \leq g$, be the unique discrete holomorphic differential with a black a_j -period δ_{jk} and vanishing white a -periods. Let ω_k^W , $1 \leq k \leq g$, be the unique discrete holomorphic differential with a white a_j -period δ_{jk} and vanishing black a -periods. We refer to the basis of these $2g$ discrete differentials as the *canonical basis of discrete holomorphic differentials*.

We define the $(g \times g)$ -matrices $\Pi^{B,B}, \Pi^{W,B}, \Pi^{B,W}, \Pi^{W,W}$ with entries

$$\Pi_{jk}^{B,B} := 2 \int_{Bb_j} \omega_k^B, \quad \Pi_{jk}^{W,B} := 2 \int_{Wb_j} \omega_k^B, \quad \Pi_{jk}^{B,W} := 2 \int_{Bb_j} \omega_k^W, \quad \Pi_{jk}^{W,W} := 2 \int_{Wb_j} \omega_k^W.$$

The *complete discrete period matrix* is the $(2g \times 2g)$ -matrix defined by

$$\tilde{\Pi} := \begin{pmatrix} \Pi^{B,W} & \Pi^{B,B} \\ \Pi^{W,W} & \Pi^{W,B} \end{pmatrix}.$$

We also define the continuous period matrix Π_Σ of Σ using the same basis of homology. However, it is the discrete period matrix $\Pi = (\Pi^{B,W} + \Pi^{B,B} + \Pi^{W,W} + \Pi^{W,B})/2$ that we mainly compare with Π_Σ . Π can be directly defined using discrete differentials with equal black and white a -periods.

Definition. The unique set of g discrete holomorphic differentials ω_k satisfying $2 \int_{Ba_j} \omega_k = \delta_{jk}$ and $2 \int_{Wa_j} \omega_k = \delta_{jk}$ for all $1 \leq j, k \leq g$ is called the *canonical set*. The $(g \times g)$ -matrix $(\Pi_{jk})_{j,k=1}^g$ with entries $\Pi_{jk} = \int_{b_j} \omega_k$ is the *discrete period matrix* of the discrete Riemann surface (Σ, Λ, z) .

Example. Let us consider a discretization of a flat torus $\Sigma = \mathbb{C}/(\mathbb{Z} + \mathbb{Z}\tau)$ of modulus $\tau \in \mathbb{C}$ with $\text{Im}(\tau) > 0$. In this case, the continuous period of Σ is τ . On the medial graph X , the differential dz is globally defined and discrete holomorphic. Thus, Π is equal to the b -period of dz , which is also τ . Note that the black and white b -periods do not have to coincide if the a -periods do not coincide [9, 6].

Theorem 2.4. *The matrices Π and $\tilde{\Pi}$ are symmetric, and their imaginary parts are positive definite.*

Since the block matrices in the diagonal of a symmetric positive definite matrix are themselves symmetric and positive definite, we also have the following corollary:

Corollary 2.5. *The imaginary parts of the symmetric matrices $\Pi^{W,B}$ and $\Pi^{B,W}$ are positive definite.*

Lemma 2.6. *Assuming all quadrilaterals of (Σ, Λ) are orthodiagonal (i.e., ρ_Q is real for all $Q \in F(\Lambda)$), we have that $\Pi^{W,B}$ and $\Pi^{B,W}$ are purely imaginary, while $\Pi^{B,B}$ and $\Pi^{W,W}$ are real matrices.*

Proof. In [6], we established a connection between our definition of the discrete Hodge star on discrete one-forms and Mercat's definition given in [29]. Specifically, if ω is a discrete one-form of type \diamond defined on the oriented edges of the boundary of the face of X corresponding to Q , then the equations governing the discrete Hodge star in a discrete chart $z = z_Q$ are given by:

$$\int_e \star \omega = \cot(\phi_Q) \int_e \omega - \frac{|z(e)|}{|z(e^*)| \sin(\phi_Q)} \int_{e^*} \omega \quad \text{and} \quad \int_{e^*} \star \omega = \frac{|z(e^*)|}{|z(e)| \sin(\phi_Q)} \int_e \omega - \cot(\phi_Q) \int_{e^*} \omega,$$

where ϕ_Q is the angle under which the diagonals of Q intersect, and e and e^* are oriented edges parallel to the black and white diagonal of Q , respectively, with $\text{Im}(e^*/e) > 0$.

For orthodiagonal quadrilaterals where ρ_Q is real, $\phi_Q = \pi/2$, simplifying the equations to:

$$\int_e \star \omega = -\frac{|z(e)|}{|z(e^*)|} \int_{e^*} \omega \quad \text{and} \quad \int_{e^*} \star \omega = \frac{|z(e^*)|}{|z(e)|} \int_e \omega.$$

In particular, if ω is a discrete one-form that is zero on white edges, then $\star \omega$ is zero on black edges, and vice versa. Additionally, if ω is real, then $\star \omega$ is also real.

Consider a discrete holomorphic differential ω and let α be the discrete one-form that is zero on white edges and agrees with ω on black edges. We define $\beta := \omega - \alpha$, which is zero on black edges. Both α and β are of type \diamond . From $\omega = -i \star \omega$, we have $\star \alpha + \star \beta = -i\alpha - i\beta$. Since only $\star \alpha$ and $-i\beta$ are non-zero on white edges, we find that $\beta = i \star \alpha$.

We have $d\alpha + id \star \alpha = d\omega = 0$. Given that α is zero on white edges and $\star \alpha$ on black edges, we can apply discrete Stokes' theorem to conclude that $d\alpha$ is zero on faces of the medial graph corresponding to white vertices, and $d \star \alpha$ is zero on faces corresponding to black vertices. This implies $d\alpha = d \star \alpha = 0$. Thus, α is a discrete harmonic form. Moreover, since $\star \bar{\alpha} = \overline{\star \alpha}$, both $\text{Re } \alpha$ and $\text{Im } \alpha$ are discrete harmonic forms as well. This implies that $\omega = \varrho + \iota$, where

$$\varrho := \text{Re } \alpha + i \star \text{Re } \alpha, \quad \iota := i \text{Im } \alpha - \star \text{Im } \alpha.$$

The forms ϱ and ι are both discrete holomorphic. The black periods of ϱ correspond to the real parts of the black periods of ω , while the white periods of ϱ correspond to i times the imaginary parts of the white periods of ω . Similarly, the white periods of ι correspond to the real parts of the white periods of ω , and the black periods of ι correspond to i times the imaginary parts of the real periods of ω .

Let $\omega = \omega_k^B$, $1 \leq k \leq g$, be the unique discrete holomorphic differential with a black a_j -period of δ_{jk} and vanishing white a -periods. According to our previous considerations, $\varrho = \varrho_k^B$ is a discrete holomorphic differential with the same black and white a -periods as ω_k^B . Therefore, by Theorem 2.3, we have

$$\omega_k^B = \varrho_k^B = \text{Re } \alpha_k^B + i \star \text{Re } \alpha_k^B.$$

Hence, the black b -periods of ω_k^B are real, and its white b -periods are purely imaginary. We can conclude that $\text{Re } \Pi^{W,B} = 0 = \text{Im } \Pi^{B,B}$. Similarly, we have $\text{Re } \Pi^{B,W} = 0 = \text{Im } \Pi^{W,W}$. \square

2.4 Discrete Dirichlet energy as a quadratic form

In Section 3, we will use the same underlying idea as Bobenko and Skopenkov in [9] to analyze the convergence of the discrete period matrix. We deduce the convergence of the discrete period matrix from the convergence of the discrete Dirichlet energy of discrete harmonic differentials with given periods (or equivalently, of discrete harmonic functions on the universal cover $(\tilde{\Sigma}, \tilde{\Lambda})$ with given periods). To do this, we represent both the continuous and discrete Dirichlet energy of continuous and discrete harmonic differentials as a quadratic form in the vector of real a - and b -periods.

Before we continue, let us review the definition of the discrete gradient by Skopenkov in [32] and relate it to the discrete differential.

Definition. Let $Q \in F(\Lambda)$ and f be a real function on its vertices. In a chart $z = z_Q$ of Q , we define the *discrete gradient* $\nabla_Q f$ as the unique vector that satisfies, for all edges e of F_Q :

$$\nabla_Q f \cdot z(e) = \int_e df.$$

Remark. The discrete gradient of a multi-valued function on $V(\tilde{\Lambda})$ is a well-defined function on $F(\Lambda)$.

In the case of a smooth function $F : U \subset \mathbb{C} \rightarrow \mathbb{R}$, an elementary calculation shows that $4|\partial F| = |\nabla F|$, such that $\langle dF, dF \rangle = \int |\nabla F|^2$. The same is true in the discrete setting.

Lemma 2.7. *Let $Q \in F(\Lambda)$ and f be a real function on its vertices. In a chart $z = z_Q$ of Q , we have*

$$\iint_{F(Q)} df \wedge \star d\bar{f} = \|\nabla_Q f\|^2 \text{area}(Q).$$

Proof. Using $df = \partial_\Lambda f dz + \bar{\partial}_\Lambda f d\bar{z}$, we compute

$$\iint_{F(Q)} df \wedge \star d\bar{f} = 4|\partial_\Lambda f|^2 \text{area}(Q).$$

On the other hand, let us integrate $\nabla_Q f$ over Q . We obtain a linear function F on Q that we restrict to a function f' on the vertices of Q . By definition of the discrete gradient, we have $df = df'$. We have seen in our previous work [5] that $\partial_\Lambda f'$ agrees with the smooth derivative. In particular,

$$4|\partial_\Lambda f| = 4|\partial_\Lambda f'| = 4|\partial F| = |\nabla F| = |\nabla_Q f|. \quad \square$$

We introduce the scalar product and norm associated with the discrete Dirichlet energy for real multi-valued functions on the discrete Riemann surface (Σ, Λ) . Using Lemma 2.7, we define the positive definite scalar product and norm as follows:

$$a(f, g) := \langle df, dg \rangle = \sum_{Q \in F(\Lambda)} \int_Q \nabla_Q f \cdot \nabla_Q g,$$

$$|f| := \sqrt{a(f, f)}.$$

In the case of smooth multi-valued functions $F, G : \tilde{\Sigma} \rightarrow \mathbb{R}$, we can also define $a(F, G)$ by replacing the discrete gradient with the smooth gradient. The norm $|F|^2$ corresponds to the Dirichlet energy of F . Additionally, $a(f, F)$ is well-defined.

It is worth noting that we omit the dependence of the scalar product a on Λ since it is already encoded in the discrete functions. Furthermore, a is derived from an inner product of the gradients, ensuring that the Cauchy-Schwarz inequality holds true.

Next, we state the representation lemma in the continuous setting, as presented in [9] (with the off-diagonal blocks interchanged). The proof of this lemma follows a similar structure to the proof of the corresponding discrete lemma, which we will present afterwards.

Lemma 2.8. Let Ω denote the unique holomorphic differential on Σ with real parts of its a - and b -periods given by $\mathcal{A}_1, \dots, \mathcal{A}_g$ and $\mathcal{B}_1, \dots, \mathcal{B}_g$, respectively. The corresponding smooth real harmonic function with these periods can be expressed as $U = \int \operatorname{Re}(\Omega)$, up to a choice of integration constant. We consider the vector $P = (\mathcal{A}_1, \dots, \mathcal{A}_g, \mathcal{B}_1, \dots, \mathcal{B}_g)^T \in \mathbb{R}^{2g}$. Then, the Dirichlet energy $\langle \Omega, \Omega \rangle = 2\langle dU, dU \rangle = 2\|U\|^2$ can be represented as a quadratic form in terms of the period matrix Π_Σ :

$$\langle \Omega, \Omega \rangle = P^T E_\Sigma P := P^T \begin{pmatrix} 2 \operatorname{Re} \Pi_\Sigma (\operatorname{Im} \Pi_\Sigma)^{-1} \operatorname{Re} \Pi_\Sigma + 2 \operatorname{Im} \Pi_\Sigma & -2 \operatorname{Re} \Pi_\Sigma (\operatorname{Im} \Pi_\Sigma)^{-1} \\ -2 (\operatorname{Im} \Pi_\Sigma)^{-1} \operatorname{Re} \Pi_\Sigma & 2 (\operatorname{Im} \Pi_\Sigma)^{-1} \end{pmatrix} P.$$

Lemma 2.9. Let ω be the unique discrete holomorphic differential on (Σ, Λ) with real parts of its black a - and b -periods given by $\mathcal{A}_1^B, \dots, \mathcal{A}_g^B$ and $\mathcal{B}_1^B, \dots, \mathcal{B}_g^B$, and real parts of its white a - and b -periods given by $\mathcal{A}_1^W, \dots, \mathcal{A}_g^W$ and $\mathcal{B}_1^W, \dots, \mathcal{B}_g^W$. The corresponding multi-valued discrete real harmonic function u with these periods can be expressed as $du = \operatorname{Re}(\omega)$, where we make a choice of two integration constants on Γ and Γ^* . We consider the vector $P' = (\mathcal{A}_1^W, \dots, \mathcal{A}_g^W, \mathcal{A}_1^B, \dots, \mathcal{A}_g^B, \mathcal{B}_1^B, \dots, \mathcal{B}_g^B, \mathcal{B}_1^W, \dots, \mathcal{B}_g^W)^T \in \mathbb{R}^{4g}$. Then, the discrete Dirichlet energy $\langle \omega, \omega \rangle = 2\langle u, u \rangle = 2\|u\|^2$ can be represented as a quadratic form in terms of the complete discrete period matrix $\tilde{\Pi}$:

$$\langle \omega, \omega \rangle = P'^T E_\Lambda P' := P'^T \begin{pmatrix} \operatorname{Re} \tilde{\Pi} (\operatorname{Im} \tilde{\Pi})^{-1} \operatorname{Re} \tilde{\Pi} + \operatorname{Im} \tilde{\Pi} & -\operatorname{Re} \tilde{\Pi} (\operatorname{Im} \tilde{\Pi})^{-1} \\ -(\operatorname{Im} \tilde{\Pi})^{-1} \operatorname{Re} \tilde{\Pi} & (\operatorname{Im} \tilde{\Pi})^{-1} \end{pmatrix} P'.$$

Proof. Clearly, $2du = 2\operatorname{Re} \omega = \omega + \bar{\omega}$. Hence, $4\langle du, du \rangle = \langle \omega, \omega \rangle + \langle \omega, \bar{\omega} \rangle + \langle \omega, \bar{\omega} \rangle + \langle \bar{\omega}, \bar{\omega} \rangle = 2\langle \omega, \omega \rangle$, which follows from the fact that $\langle \bar{\omega}, \bar{\omega} \rangle = \overline{\langle \omega, \omega \rangle} = \langle \omega, \omega \rangle$ and $\omega \wedge \star \omega = -i\omega \wedge \omega = 0$.

Let us consider the black and white a - and b -periods of ω , denoted by A_k^B, B_k^B and A_k^W, B_k^W respectively, where $1 \leq k \leq g$. Since ω is a discrete holomorphic differential, we have $\star \omega = -i\omega$. Applying the discrete Riemann bilinear identity to the closed differentials ω and $\bar{\omega}$, we obtain:

$$\begin{aligned} \langle \omega, \omega \rangle &= \iint_{F(X)} \omega \wedge \star \bar{\omega} = i \iint_{F(X)} \omega \wedge \bar{\omega} \\ &= \frac{i}{2} \sum_{k=1}^g (A_k^B \bar{B}_k^W - B_k^B \bar{A}_k^W) + \frac{i}{2} \sum_{k=1}^g (A_k^W \bar{B}_k^B - B_k^W \bar{A}_k^B) \\ &= \sum_{k=1}^g (\operatorname{Re} A_k^B \operatorname{Im} B_k^W - \operatorname{Im} A_k^B \operatorname{Re} B_k^W + \operatorname{Re} A_k^W \operatorname{Im} B_k^B - \operatorname{Im} A_k^W \operatorname{Re} B_k^B). \end{aligned}$$

The complete discrete period matrix relates the b -periods of ω to its a -periods. By rewriting the corresponding system of equations, we can express the imaginary parts $\operatorname{Im} A_k^B, \operatorname{Im} A_k^W, \operatorname{Im} B_k^W, \operatorname{Im} B_k^B$ in terms of their corresponding real parts $\operatorname{Re} A_k^B = \mathcal{A}_k^B, \operatorname{Re} A_k^W = \mathcal{A}_k^W, \operatorname{Re} B_k^W = \mathcal{B}_k^W, \operatorname{Re} B_k^B = \mathcal{B}_k^B$.

Consider the canonical basis of discrete holomorphic differentials $\omega_1^W, \dots, \omega_g^W, \omega_1^B, \dots, \omega_g^B$. We can express ω in this basis as a linear combination: $\omega = \sum_{k=1}^g (A_k^W \omega_k^W + A_k^B \omega_k^B)$. Now, let us introduce the g -dimensional vectors $A_W := (A_1^W, \dots, A_g^W)^T$, $A_B := (A_1^B, \dots, A_g^B)^T$, $B_W := (B_1^W, \dots, B_g^W)^T$, $B_B := (B_1^B, \dots, B_g^B)^T$, and the $2g$ -dimensional vectors $A := (A_W^T, A_B^T)^T$ and $B := (B_B^T, B_W^T)^T$. Note that $P'^T = \operatorname{Re}(A^T, B^T)$. Thus, we can express B as follows:

$$B = \begin{pmatrix} B_B \\ B_W \end{pmatrix} = \begin{pmatrix} \Pi^{B,W} A_W + \Pi^{B,B} A_B \\ \Pi^{W,B} A_B + \Pi^{W,W} A_W \end{pmatrix} = \begin{pmatrix} \Pi^{B,W} & \Pi^{B,B} \\ \Pi^{W,W} & \Pi^{W,B} \end{pmatrix} \begin{pmatrix} A_W \\ A_B \end{pmatrix} = \tilde{\Pi} A.$$

Now, let us proceed with the calculations. We have:

$$\operatorname{Re} B = \operatorname{Re} \tilde{\Pi} \operatorname{Re} A - \operatorname{Im} \tilde{\Pi} \operatorname{Im} A \Rightarrow \operatorname{Im} A = \left(\operatorname{Im} \tilde{\Pi} \right)^{-1} \operatorname{Re} \tilde{\Pi} \operatorname{Re} A - \left(\operatorname{Im} \tilde{\Pi} \right)^{-1} \operatorname{Re} B,$$

$$\operatorname{Im} B = \operatorname{Re} \tilde{\Pi} \operatorname{Im} A + \operatorname{Im} \tilde{\Pi} \operatorname{Re} A \Rightarrow \operatorname{Im} B = \left(\operatorname{Re} \tilde{\Pi} \left(\operatorname{Im} \tilde{\Pi} \right)^{-1} \operatorname{Re} \tilde{\Pi} + \operatorname{Im} \tilde{\Pi} \right) \operatorname{Re} A - \operatorname{Re} \tilde{\Pi} \left(\operatorname{Im} \tilde{\Pi} \right)^{-1} \operatorname{Re} B.$$

By substituting these expressions into the equation obtained from the discrete Riemann bilinear identity, we obtain:

$$\begin{aligned} \langle \omega, \omega \rangle &= \sum_{k=1}^g \left(\operatorname{Re} A_k^B \operatorname{Im} B_k^W - \operatorname{Im} A_k^B \operatorname{Re} B_k^W + \operatorname{Re} A_k^W \operatorname{Im} B_k^B - \operatorname{Im} A_k^W \operatorname{Re} B_k^B \right) = \operatorname{Re} A^T \operatorname{Im} B - \operatorname{Re} B^T \operatorname{Im} A \\ &= \operatorname{Re} A^T \left(\operatorname{Re} \tilde{\Pi} \left(\operatorname{Im} \tilde{\Pi} \right)^{-1} \operatorname{Re} \tilde{\Pi} + \operatorname{Im} \tilde{\Pi} \right) \operatorname{Re} A - \operatorname{Re} A^T \operatorname{Re} \tilde{\Pi} \left(\operatorname{Im} \tilde{\Pi} \right)^{-1} \operatorname{Re} B \\ &\quad - \operatorname{Re} B^T \left(\operatorname{Im} \tilde{\Pi} \right)^{-1} \operatorname{Re} \tilde{\Pi} \operatorname{Re} A + \operatorname{Re} B^T \left(\operatorname{Im} \tilde{\Pi} \right)^{-1} \operatorname{Re} B \\ &= \left(\operatorname{Re} A^T, \operatorname{Re} B^T \right) \begin{pmatrix} \operatorname{Re} \tilde{\Pi} \left(\operatorname{Im} \tilde{\Pi} \right)^{-1} \operatorname{Re} \tilde{\Pi} + \operatorname{Im} \tilde{\Pi} & - \operatorname{Re} \tilde{\Pi} \left(\operatorname{Im} \tilde{\Pi} \right)^{-1} \\ - \left(\operatorname{Im} \tilde{\Pi} \right)^{-1} \operatorname{Re} \tilde{\Pi} & \left(\operatorname{Im} \tilde{\Pi} \right)^{-1} \end{pmatrix} \begin{pmatrix} \operatorname{Re} A \\ \operatorname{Re} B \end{pmatrix} = P'^T E_\Lambda P'. \quad \square \end{aligned}$$

Note that E_Σ includes a factor of 2 that is not present in E_Λ due to the discrete Riemann bilinear identity having a factor of 1/2, which is absent in the smooth case.

3 Convergence of the discrete Dirichlet energy

This chapter focuses on proving the convergence of the discrete Dirichlet energy of a discrete harmonic differential, which has prescribed a - and b -periods (with black and white periods being equal), to the continuous Dirichlet energy of the corresponding smooth harmonic differential with the same prescribed periods. The theorem stating this convergence is presented in Section 3.5, along with a discussion of its implications for the related quadratic form. While these theorems hold true for general discrete Riemann surfaces, the convergence of the corresponding multi-valued discrete harmonic functions to their continuous counterparts is only established in the case of orthodiagonal discrete Riemann surfaces. We will outline how the proof given by Bobenko and Skopenkov in [9] for Delaunay-Voronoi quadrangulations can be adapted to our more general setting.

Before diving into the proof, we provide some geometric preliminaries in Section 3.1. Specifically, we adapt the concept of h -adaptedness introduced in [4] to our quad-graph framework. This adaptation ensures a linear rate of convergence. In contrast, in the general case, the convergence rate depends on the orders of conical singularities. Section 3.2 covers the basic notation and outlines our proof strategy. We draw inspiration from nonconforming finite elements [10] and base our proof on the Second Lemma of Strang. We discuss the approximation and consistency errors separately in Sections 3.3 and 3.4.

3.1 Geometric preliminaries

To establish the convergence of the discrete Dirichlet energy and the discrete period matrix, it is essential to have bounded interior angles and intersection angles of diagonals in quadrilaterals. We introduce the concept of ϕ -regularity to ensure this boundedness.

Definition. We define a discrete Riemann surface (Σ, Λ) to be ϕ -regular if the interior angles of all quadrilaterals $Q \in F(\Lambda)$ are bounded from below by ϕ , and the intersection angle between the diagonals of each quadrilateral lies in the interval $[\phi, \pi - \phi]$. In other words, we require that $|\arg(\rho_Q)| \leq \frac{\pi}{2} - \phi$, where $\arg(\rho_Q) \in (-\pi, \pi]$ denotes the argument of the complex number ρ_Q .

Throughout our analysis, we will assume that (Σ, Λ) is ϕ -regular.

In the upcoming sections, we will observe that the presence of conical singularities with a total angle of 4π or more leads to a slower rate of convergence. In order to achieve the same linear convergence rate $O(h)$ as when such singularities do not exist, we need to consider *adapted* cell decompositions Λ . This notion is inspired by the work of Bobenko and Bücking in [4] for triangulations.

Definition. We say that a discrete Riemann surface (Σ, Λ) is h -adapted if its maximum edge length is h . Moreover, for any conical singularity $O \in S$ with $\gamma_O \leq 1/2$, we require that $|g_O(x) - g_O(y)| \leq h$ for any edge $xy \in E(\Lambda) \cap D_O$ within the chart (D_O, g_O) defined in Section 2.1.

Let $xy \in E(\Lambda) \cap D_O$ be an edge, where x and y are points on the discrete Riemann surface (Σ, Λ) . Assuming that x is closer to the conical singularity O than y , i.e., $|Ox| \leq |Oy|$, we address a correction to the claim made in [4] regarding h -adaptedness and the inequality $|xy| \leq h|Ox|^{1-\gamma_O}$. The presence of the mapping function g_O , which scales the angle $\angle xOy$ by the factor $\gamma_O \leq 1/2$, complicates the relationship between $|xy|$ and $|g_O(x) - g_O(y)|$.

If $\angle xOy$ is small and $|Oy| = |Ox| < 1$ approaches 1, we observe that $|g_O(x) - g_O(y)| \approx \gamma_O|xy|$ due to the approximation $\sin(\alpha) \approx \alpha$ for small $\alpha > 0$. As a result, if we impose the condition $|g_O(x) - g_O(y)| = h$, it would imply $|xy| \approx h\gamma_O^{-1} > h|Ox|^{1-\gamma_O}$. Therefore, we present a corrected version of the claim.

Lemma 3.1. *Let $\gamma_O \leq 1/2$ and consider an edge $xy \in E(\Lambda) \cap D_O$ on the discrete Riemann surface (Σ, Λ) , such that $|Ox| \leq |Oy|$. Then, we have the inequality:*

$$|xy| \leq \left(1 + \frac{\pi}{2\gamma_O}\right) h|Ox|^{1-\gamma_O}.$$

Proof. In polar coordinates (r, ψ) , we have $g_O(r, \psi) = r^{\gamma_O} \exp(i\gamma_O\psi)$. We will estimate the radial and angular components of $|xy|$ separately and use the triangle inequality to derive a bound for $|xy|$.

For the radial component, we have:

$$\begin{aligned} h &\geq |g_O(x) - g_O(y)| \geq |Oy|^{\gamma_O} - |Ox|^{\gamma_O} \geq |Oy| \cdot |Ox|^{\gamma_O-1} - |Ox|^{\gamma_O} \\ &\Rightarrow h|Ox|^{1-\gamma_O} \geq |Oy| - |Ox| \end{aligned}$$

Next, we consider the angle component. Since $\gamma_O \leq 1/2$, we have $\gamma_O\alpha := \gamma_O|\angle xOy| \leq \pi/2$. Thus, $\sin(\gamma_O\alpha/2) \geq \gamma_O\alpha/\pi$. Since $|Ox| \leq |Oy|$, the edge $g_O(x)g_O(y)$ is not smaller than the chord corresponding to the angle $\gamma_O\alpha$ and the radius $|Ox|^{\gamma_O}$. Therefore, we have:

$$\begin{aligned} h &\geq |g_O(x) - g_O(y)| \geq 2|Ox|^{\gamma_O} \sin\left(\frac{\gamma_O\alpha}{2}\right) \geq 2|Ox|^{\gamma_O} \frac{\gamma_O\alpha}{\pi} \\ &\Rightarrow 2|Ox| \sin\left(\frac{\alpha}{2}\right) \leq |Ox|\alpha \leq |Ox|^{1-\gamma_O} h \frac{\pi}{2\gamma_O}. \end{aligned}$$

Combining the bounds for the radial and angular components, we apply the triangle inequality to obtain:

$$|xy| \leq (|Oy| - |Ox|) + 2|Ox| \sin\left(\frac{\alpha}{2}\right) \leq \left(1 + \frac{\pi}{2\gamma_O}\right) h|Ox|^{1-\gamma_O}. \quad \square$$

In our proof, we will primarily focus on the case of general discrete Riemann surfaces, and provide brief comments on the relatively minor modifications required for the case of h -adaptedness.

3.2 Notation and strategy of proof

We introduce some notation for the rest of this chapter. Let h denote the maximum edge length of a discrete Riemann surface (Σ, Λ) . We will always assume that (Σ, Λ) is ϕ -regular.

Consider a fixed vector of periods $P \in \mathbb{R}^{2g}$. We define U to be a multi-valued smooth harmonic function with its a - and b -periods given by P . Similarly, u is a multi-valued discrete harmonic function with its black and white a - and b -periods equal to P , where the corresponding black and white periods coincide. U_Λ represents the restriction of U to $V(\tilde{\Lambda})$, and it is a multi-valued discrete function with equal black and white periods that match those of u .

Let M_P be the set of all multi-valued functions $f : V(\tilde{\Lambda}) \rightarrow \mathbb{R}$ with the same periods as u , and let M_0 be the set of all functions $f : V(\Lambda) \rightarrow \mathbb{R}$.

In their work [9], Bobenko and Skopenkov considered triangulations Γ of Σ and the dual lattice Γ^* consisting of the circumcenters of triangles. The quadrilateral cell decomposition Λ was defined by the black vertices $V(\Gamma)$ and the white vertices $V(\Gamma^*)$, where the vertices of a triangle were connected to the dual vertex of that triangle. They observed that, just as in our case, the discrete Dirichlet energy of a discrete function coincided with the Dirichlet energy of its linear interpolation on Γ . However, a crucial difference is that their interpolation was a continuous function, which allowed for a direct comparison with the smooth Dirichlet energy. In our setting, where the interpolations are piecewise linear and non-continuous, we need to employ different techniques. We draw inspiration from nonconforming finite element methods, specifically Braess' analysis on Crouzeix-Raviart elements or nonconforming P_1 elements [10]. These finite elements correspond to triangulations and provide a discretization of the Poisson equation in a planar domain with boundary, estimating the difference between the discrete and actual solutions in terms of the Dirichlet energy norm. We adapt these ideas to our context, incorporating a careful analysis near the singularities of Σ , as done by Bobenko and Skopenkov.

We now introduce our version of the Second Lemma of Strang, also known as the Lemma of Berger, Scott, and Strang (Lemma 1.2 in Chapter III of [10]). The first term in the inequality corresponds to the *approximation error*, while the second term corresponds to the *consistency error*. Since $U_\Lambda \in M_P$, we can choose $v = U_\Lambda$ to bound the approximation error.

Lemma 3.2.

$$\|U - u\| \leq 2 \inf_{v \in M_P} \|U - v\| + \sup_{f \in M_0} \frac{|a(U, f)|}{\|f\|}$$

Proof. Corollary 2.2 implies that $a(u, u - v) = \langle du, df \rangle = 0$ with $f := u - v \in M_0$. Thus, we have

$$\begin{aligned} \|u - v\|^2 &= a(u - v, u - v) = a(U - v, u - v) + a(u, u - v) - a(U, u - v) \\ &= a(U - v, u - v) - a(U, u - v) \\ \Rightarrow \|u - v\| &= \frac{a(U - v, u - v)}{\|u - v\|} - \frac{a(U, u - v)}{\|u - v\|} \leq \|U - v\| + \frac{|a(U, f)|}{\|f\|} \end{aligned}$$

by the Cauchy-Schwarz inequality. Applying the triangle inequality, we obtain for any $v \in M_P$:

$$\|U - u\| \leq \|U - v\| + \|u - v\| \leq 2\|U - v\| + \frac{|a(U, f)|}{\|f\|}. \quad \square$$

In the forthcoming approximations, we will encounter various constants that depend on parameters such as the smooth function U , the regularity parameter ϕ , or the singularity $O \in S$. To simplify the notation, we denote these constants by $C_{a,b,c}^{(i)}$, where i indexes the constants and a, b, c represent the corresponding parameters. For example, $C_{U,O}^{(1)}$ depends solely on the smooth function U and the singularity $O \in S$ and is the first constant introduced in the subsequent analysis. It is essential to note that all these constants depend on the polyhedral surface Σ without any further specification.

To distinguish the constants in the h -adapted case, we denote them by $C_{a,b,c}^{(i,h)}$. Although we do not provide explicit expressions for these constants here, it is important to note that we have designed the proofs in a way that allows for easy computation of these constants.

In our subsequent local investigations, we will work with charts to facilitate our analysis. Recall that a discrete chart z_Q of a quadrilateral face $Q \in F(\Lambda)$ is defined as an isometric embedding of Q into

the complex plane \mathbb{C} . To simplify the notation, we identify the vertices and edges of Q with their corresponding complex values. In cases where Q is not incident to a singularity $O \in S$, we extend the chart z_Q to an isometric mapping g of a neighborhood around Q to \mathbb{C} . For the sake of simplicity, we denote the composition $U \circ g^{-1}$ as U in our discussions. In this context, gradients such as ∇U and $\nabla_Q u$ may depend on the choice of chart, but their lengths $|\nabla U|$, $|\nabla_Q u|$, and $|\nabla U - \nabla_Q u|$ are independent of the specific chart chosen.

Finally, for simplicity, we introduce the notation $|x|_0 := \max\{0, x\}$.

3.3 The approximation error

To bound the approximation error, we follow the approach outlined by Bobenko and Skopenkov in [9], with the adaptations for h -adapted discrete Riemann surfaces provided by Bobenko and Bücking in [4].

Let us first recall the projection lemma, which is a minor variant of Lemma 4.2 in [32, 9]:

Lemma 3.3. *Let $x_1, x_2 \in \mathbb{C} \cong \mathbb{R}^2$ be two linearly independent vectors of length one, and let the angle $\alpha := \min \arccos(\pm x_1 \cdot x_2)$ be the smaller angle between x_1 and $\pm x_2$. Then, for any $y \in \mathbb{C}$, we have*

$$|y| \leq \frac{2}{\sin(\alpha)} \max_{i \in \{1,2\}} |x_i \cdot y|.$$

Proof. Without loss of generality, we can assume that $x_1 \cdot x_2 \geq 0$. Let $\beta_i := \arccos(x_i \cdot y/|y|)$. Then, $\alpha = \pm\beta_1 \pm \beta_2$ for an appropriate choice of signs.

Since $\alpha \leq \frac{\pi}{2}$, it follows that not both β_1 and β_2 can be in the interval $(\frac{\pi-\alpha}{2}, \frac{\pi+\alpha}{2})$. Let us assume that β_i is not in this interval. Then, we have:

$$|x_i \cdot y| = |y| \cdot |\cos(\beta_i)| \geq |y| \cos\left(\frac{\pi-\alpha}{2}\right) = |y| \sin\left(\frac{\alpha}{2}\right) \geq |y| \frac{\sin(\alpha)}{2}. \quad \square$$

Next, we introduce the following definition:

Definition. Let $F : U \subset \mathbb{C} \rightarrow \mathbb{R}$. We define $|D^k F(x + iy)| := \max_{0 \leq j \leq k} \left| \frac{\partial^k F}{\partial x \partial^{k-j} y}(x + iy) \right|$.

Now, we can state the gradient approximation lemma, which is an analogue of Lemma 4.3 in [9] or Lemma 4.5 in [32]. The main difference is that we consider quadrilaterals that may be non-convex, and we do not consider their convex hull since it may contain a conical singularity.

Lemma 3.4. *Let $Q \in F(\Lambda)$ be not incident to a conical singularity of Σ . Then, we have:*

$$\max_{z \in Q} |\nabla U(z) - \nabla_Q U_\Lambda| \leq \frac{8\sqrt{2}}{\sin(\phi)} h \max_{z \in Q} \|D^2 U(z)\|.$$

Proof. Consider the quadrilateral Q with vertices b_-, w_-, b_+, w_+ in counterclockwise order. Let e denote one of the two diagonals b_-b_+ and w_-w_+ . We will analyze two cases.

In the case that e is contained in Q , we integrate the expression $(\nabla U(z') - \nabla_Q U_\Lambda) \cdot e/|e|$ along e and apply Rolle's theorem. This yields a point $z_0 \in e$ where $(\nabla U(z_0) - \nabla_Q U_\Lambda) \cdot e/|e| = 0$. By using the bound $|\nabla U(z') - \nabla U(z_0)| \leq 4\sqrt{2}h \max_{z \in Q} \|D^2 U(z)\|$, we obtain for all $z' \in Q$ the inequality

$$\frac{|(\nabla U(z') - \nabla_Q U_\Lambda) \cdot e|}{|e|} \leq 4\sqrt{2}h \max_{z \in Q} \|D^2 U(z)\|.$$

In the case where e is not contained inside Q , we assume that the reflex angle is at w_- . We consider the path $b_-w_-b_+$ and integrate $(\nabla U(z') - \nabla_Q U_\Lambda) \cdot (w_- - b_-)/|w_- - b_-|$ along b_-w_- and $(\nabla U(z') - \nabla_Q U_\Lambda) \cdot (b_+ - w_-)/|b_+ - w_-|$ along w_-b_+ . This results in a piecewise linear function that takes the same value at

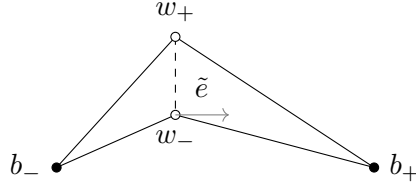


Figure 3: Application of (generalized) Rolle's theorem if Q is not convex.

b_- and b_+ . By applying the generalized Rolle's theorem, we can find a point z_0 on b_-w_- or b_+w_- where $(\nabla U(z_0) - \nabla_Q U_\Lambda) \cdot (w_- - b_-)/|w_- - b_-| = 0$, or

$$(\nabla U(w_-) - \nabla_Q U_\Lambda) \cdot \frac{w_- - b_-}{|w_- - b_-|} \geq 0 \geq (\nabla U(w_-) - \nabla_Q U_\Lambda) \cdot \frac{b_+ - w_-}{|b_+ - w_-|}$$

or the inequality with reversed signs holds true. In either case, there exist $z_0 \in b_-w_-b_+$ and a unit vector \tilde{e} whose argument lies between those of $(w_- - b_-)$ and $(b_+ - w_-)$, such that $(\nabla U(z_0) - \nabla_Q U_\Lambda) \cdot \tilde{e} = 0$. As before, we obtain the inequality

$$|(\nabla U(z') - \nabla_Q U_\Lambda) \cdot \tilde{e}| \leq 4\sqrt{2}h \max_{z \in Q} \|D^2 U(z)\|$$

for all $z' \in Q$. Thus, we have established the inequality

$$|(\nabla U(z') - \nabla_Q U_\Lambda) \cdot x_i| \leq 4\sqrt{2}h \max_{z \in Q} \|D^2 u(z)\|$$

for two unit vectors x_1, x_2 (either $e/|e|$ or \tilde{e} for each of the two diagonals). Due to the construction and ϕ -regularity, the angle between x_1 and x_2 falls within the range of ϕ to $\pi - \phi$. Thus, we can apply Lemma 3.3 to deduce

$$|\nabla U(z') - \nabla_Q U_\Lambda| \leq \frac{8\sqrt{2}}{\sin(\phi)} h \max_{z \in Q} \|D^2 u(z)\|. \quad \square$$

Definition. Let $O \in \Sigma$ be a conical singularity or a regular point of Σ . We consider the domain D_O of the chart g_O as defined in Section 2.1. In this context, we define the functions $U_O := U \circ g_O^{-1}$ and $U_p := U \circ g_p^{-1}$ for any $p \in D_O \setminus O$.

In the subsequent analysis, we fix a point $O \in \Sigma$. Recall that the radius of D_O was denoted by R_O . Our goal is to establish results analogous to Lemmas 4.5 to 4.13 presented in the work of Bobenko and Skopenkov [9]. While we largely follow their proof ideas, we make slight adjustments to accommodate our framework involving quadrilaterals. The lack of boundedness in the partial derivatives of g_p near O prevents us from directly applying Lemma 3.4 to prove the convergence of the discrete Dirichlet energy.

Lemma 3.5. *Let $p \in D_O$, $p \neq O$. Then, we have the following estimates:*

$$\begin{aligned} \|D^1 U_p(z)|_{z=g_p(p)}\| &\leq C_{U,O}^{(1)} r^{\gamma_O-1}, \\ \|D^2 U_p(z)|_{z=g_p(p)}\| &\leq C_{U,O}^{(2)} r^{\gamma_O-2}. \end{aligned}$$

Proof. Using the chain rule and the fact that $U_p = U \circ g_O^{-1} \circ g_O \circ g_p^{-1}$, we have

$$\|D^1 U_p(z)|_{z=g_p(p)}\| \leq 2 \|D^1 U_O(z)|_{z=g_O(p)}\| \cdot \|D^1 (g_O \circ g_p^{-1})(z)|_{z=g_p(p)}\|.$$

Applying Leibniz' rule, we obtain for the second derivative

$$\begin{aligned} \|D^2 U_p(z)|_{z=g_p(p)}\| &\leq 4 \|D^2 U_O(z)|_{z=g_O(p)}\| \cdot \|D^1 (g_O \circ g_p^{-1})(z)|_{z=g_p(p)}\|^2 \\ &\quad + 2 \|D^1 U_O(z)|_{z=g_O(p)}\| \cdot \|D^2 (g_O \circ g_p^{-1})(z)|_{z=g_p(p)}\|. \end{aligned}$$

By construction, the map $g_O \circ g_p^{-1}$ is of the form $z \mapsto (az)^{\gamma_O}$ with $|a| = 1$. This yields

$$\begin{aligned}\|D^1(g_O \circ g_p^{-1})(z)|_{z=g_p(p)}\| &= \gamma_O r^{\gamma_O-1}, \\ \|D^2(g_O \circ g_p^{-1})(z)|_{z=g_p(p)}\| &= \gamma_O(\gamma_O - 1)r^{\gamma_O-2}.\end{aligned}$$

Since U_O extends smoothly to a neighborhood of the disk $g_O(D_O)$ of radius R_O in \mathbb{C} , we can define $\max_{z \in g_O(\overline{D_O})} |D^k U_O(z)|$. Combining the previous results, we obtain

$$\begin{aligned}\|D^1 U_p(z)|_{z=g_p(p)}\| &\leq 2 \max_{z \in g_O(\overline{D_O})} \|D^1 U_O(z)\| \cdot \gamma_O r^{\gamma_O-1}, \\ \|D^2 U_p(z)|_{z=g_p(p)}\| &\leq 4 \max_{z \in g_O(\overline{D_O})} \|D^2 U_O(z)\| \cdot \gamma_O^2 r^{2\gamma_O-2} + 2 \max_{z \in g_O(\overline{D_O})} \|D^1 U_O(z)\| \cdot \gamma_O(\gamma_O - 1)r^{\gamma_O-2} \\ &\leq 2\gamma_O \left(2 \max_{z \in g_O(\overline{D_O})} \|D^2 U_O(z)\| \gamma_O R_O^{\gamma_O} + \max_{z \in g_O(\overline{D_O})} \|D^1 U_O(z)\| (\gamma_O - 1) \right) r^{\gamma_O-2}. \quad \square\end{aligned}$$

Lemma 3.6. *Let $Q \subset D_O$ be a quadrilateral that does not intersect the disk of radius h around O . If (Σ, Λ) is h -adapted, we change the radius to h^{1/γ_O} and assume that $\gamma_O \leq 1/2$. Then, we have the following estimates:*

$$\begin{aligned}\int_Q |\nabla U - \nabla_Q U_\Lambda|^2 &\leq C_{U,O,\phi}^{(3)} h \int_Q r^{2\gamma_O-2} dr d\psi, \\ \text{and } \int_Q |\nabla U - \nabla_Q U_\Lambda|^2 &\leq C_{u,O,\phi}^{(3,h)} h \int_Q r^{\gamma_O-1} dr d\psi \quad \text{in the } h\text{-adapted case.}\end{aligned}$$

Proof. Let $z = (r(z), \psi(z)) \in Q$ denote the vertex of Q closest to O . The distance r from any other point in Q to O satisfies $h \leq r(z) \leq r \leq r(z) + 2h \leq 3r(z)$. Combining Lemmas 3.4 and 3.5, we obtain:

$$\begin{aligned}\int_Q |\nabla U - \nabla_Q U_\Lambda|^2 &\leq \text{area}(Q) \max_{w \in Q} |\nabla U(w) - \nabla_Q U_\Lambda|^2 \\ &\leq \frac{128}{\sin^2(\phi)} h^2 \text{area}(Q) \left(C_{U,O}^{(2)} \right)^2 3^{2|\gamma_O-2|_0} r(z)^{2\gamma_O-4} \\ &\leq \frac{128 \left(C_{U,O}^{(2)} \right)^2}{\sin^2(\phi)} h 3^{2|\gamma_O-2|_0} 3^{2|2-\gamma_O|_0} \int_Q h r^{2\gamma_O-4} r dr d\psi \\ &\leq \frac{128 \left(C_{U,O}^{(2)} \right)^2}{\sin^2(\phi)} 3^{2|\gamma_O-2|} h \int_Q r^{2\gamma_O-2} dr d\psi.\end{aligned}$$

In the h -adapted case, $h^{1/\gamma_O} \leq r(z) \leq r \leq r(z) + 2 \left(1 + \frac{\pi}{2\gamma_O} \right) h r(z)^{1-\gamma_O} \leq \left(3 + \frac{\pi}{\gamma_O} \right) r(z)$ by Lemma 3.1. Noting that $\gamma_O \leq 1/2$ and $h \leq r^{\gamma_O}$ by assumption, we have

$$\begin{aligned}\int_Q |\nabla U - \nabla_Q U_\Lambda|^2 &\leq \frac{128}{\sin^2(\phi)} h^2 \left(1 + \frac{\pi}{2\gamma_O} \right)^2 r(z)^{2-2\gamma_O} \text{area}(Q) \left(C_{U,O}^{(2)} \right)^2 r(z)^{2\gamma_O-4} \\ &\leq \frac{128 \left(C_{U,O}^{(2)} \right)^2}{\sin^2(\phi)} \left(1 + \frac{\pi}{2\gamma_O} \right)^2 \left(3 + \frac{\pi}{\gamma_O} \right)^2 h \int_Q h r^{-2} r dr d\psi \\ &\leq \frac{128 \left(C_{U,O}^{(2)} \right)^2}{\sin^2(\phi)} \left(1 + \frac{\pi}{2\gamma_O} \right)^2 \left(3 + \frac{\pi}{\gamma_O} \right)^2 h \int_Q r^{\gamma_O-1} dr d\psi. \quad \square\end{aligned}$$

Lemma 3.7. Let $T' = T'_{O,h}$ and $T'_{(h)} = T'_{O,h,(h)}$ be the sets of all quadrilaterals $Q \subset D_O$ of Λ that do not intersect the disks of radius h and h^{1/γ_O} (if $\gamma_O < 1/2$, otherwise of radius h) around O , respectively. Additionally, we assume $h \leq R_O$. Then,

$$\sum_{Q \in T'} \int_Q |\nabla U - \nabla_Q U_\Lambda|^2 \leq C_{U,O,\phi}^{(4)} \lambda_O(h) := C_{U,O,\phi}^{(4)} \cdot \begin{cases} h & \text{if } \gamma_O > 1/2, \\ h \left| \log \frac{h}{R_O} \right| & \text{if } \gamma_O = 1/2, \\ h^{2\gamma_O} & \text{if } \gamma_O < 1/2. \end{cases}$$

If (Σ, Λ) is h -adapted and $\gamma_O \leq 1/2$, then

$$\sum_{Q \in T'} \int_Q |\nabla U - \nabla_Q U_\Lambda|^2 \leq C_{U,O,\phi}^{(4,h)} h.$$

Proof. Applying Lemma 3.6 to each quadrilateral $Q \in T'$ and then extending the integration domain to an annulus, we obtain the following inequalities:

$$\begin{aligned} \sum_{Q \in T'} \int_Q |\nabla U - \nabla_Q U_\Lambda|^2 &\leq C_{U,O,\phi}^{(3)} h \sum_{Q \in T'} \int_Q r^{2\gamma_O-2} dr d\psi \\ &\leq C_{U,O,\phi}^{(3)} h \int_h^{R_O} \int_0^{2\pi/\gamma_O} r^{2\gamma_O-2} dr d\psi = \frac{2\pi C_{U,O,\phi}^{(3)}}{\gamma_O} \int_h^{R_O} r^{2\gamma_O-2} dr \\ &\leq \frac{2\pi C_{U,O,\phi}^{(3)}}{\gamma_O} \cdot \begin{cases} h R_O^{2\gamma_O-1} / (2\gamma_O - 1) & \text{if } \gamma_O > 1/2, \\ h \left| \log \frac{h}{R_O} \right| & \text{if } \gamma_O = 1/2, \\ h^{2\gamma_O} / (1 - 2\gamma_O) & \text{if } \gamma_O < 1/2. \end{cases} \end{aligned}$$

For the h -adapted case:

$$\sum_{Q \in T'_{(h)}} \int_Q |\nabla U - \nabla_Q U_\Lambda|^2 \leq C_{U,O,\phi}^{(3,h)} h \int_{h^{1/\gamma_O}}^{R_O} \int_0^{2\pi/\gamma_O} r^{\gamma_O-1} dr d\psi \leq \frac{2\pi C_{U,O,\phi}^{(3,h)}}{\gamma_O^2} R_O^{\gamma_O} h. \quad \square$$

In the following, we aim to estimate the integral of $|\nabla U(z) - \nabla_Q U_\Lambda|^2$ close to the singularity O . To do this, we first find an upper bound for $|\nabla_Q U_\Lambda|^2$. By the definition of the discrete gradient and using projection Lemma 3.3, it suffices to bound the difference quotients along the diagonals of a quadrilateral.

Lemma 3.8. For any two points $x \neq y$ in D_O , we have

$$\frac{|U(x) - U(y)|}{|xy|} \leq C_{U,O}^{(5)} \max\{|Ox|, |Oy|\}^{\gamma_O-1}.$$

Proof. We use polar coordinates $p = (r, \psi)$ in D_O . By Lemma 3.5, we obtain:

$$|U(x) - U(y)| \leq \int_{xy} \sqrt{2} \|D^1 U_p(z)|_{z=g_p(p)}\| (|dr| + r|d\psi|) \leq \sqrt{2} C_{U,O}^{(1)} \int_{xy} r^{\gamma_O-1} (|dr| + r|d\psi|).$$

Without loss of generality, let us assume $|Oy| \geq |Ox|$. If the projection of O onto the line xy lies outside the segment xy , then

$$\int_{xy} r^{\gamma_O-1} |dr| \leq \frac{1}{\gamma_O} |Oy|^{\gamma_O}.$$

If the projection of O , denoted by q , lies between x and y , then

$$\int_{xy} r^{\gamma_O-1} |dr| = \frac{1}{\gamma_O} (|Oy|^{\gamma_O} + |Ox|^{\gamma_O} - 2|Oq|^{\gamma_O}) \leq \frac{2}{\gamma_O} (|Oy|^{\gamma_O} - \max\{0, |Oy| - |xy|\}^{\gamma_O}).$$

In the case that $|xy| \geq |Oy|$, we obtain

$$\begin{aligned} |U(x) - U(y)| &\leq \frac{2\sqrt{2}C_{U,O}^{(1)}}{\gamma_O} |Oy|^{\gamma_O} + \sqrt{2}C_{U,O}^{(1)} \left| \int_{xy} r^{\gamma_O} d\psi \right| \\ &\leq \frac{2\sqrt{2}C_{U,O}^{(1)}}{\gamma_O} |xy||Oy|^{\gamma_O-1} + \sqrt{2}C_{U,O}^{(1)} |xy||Oy|^{\gamma_O-1} |\angle xOy| \\ &\leq \left(\frac{2\sqrt{2}}{\gamma_O} + \sqrt{2}\pi \right) C_{U,O}^{(1)} |xy||Oy|^{\gamma_O-1}. \end{aligned}$$

If $|xy| < |Oy|$, then $|\angle xOy|$ cannot be the largest angle of the triangle $\triangle xOy$, so $|\angle xOy| < \pi/2$ and $|\angle xOy| < (\pi/2) \sin |\angle xOy|$ by the concavity of the sine function. Applying the sine theorem, we have $|Oy| \sin |\angle xOy| \leq |xy|$. By using Bernoulli's inequality for $\gamma_O < 1$ and the monotonicity of the power function for $\gamma_O \geq 1$, we get

$$|Oy|^{\gamma_O} - (|Oy| - |xy|)^{\gamma_O} = |Oy|^{\gamma_O} (1 - (1 - |xy|/|Oy|)^{\gamma_O}) \leq \max\{1, \gamma_O\} |xy||Oy|^{\gamma_O-1}.$$

Hence,

$$\begin{aligned} |U(x) - U(y)| &\leq \frac{2\sqrt{2}C_{U,O}^{(1)}}{\gamma_O} \max\{1, \gamma_O\} |xy||Oy|^{\gamma_O-1} + \sqrt{2}C_{U,O}^{(1)} |Oy|^{\gamma_O} |\angle xOy| \\ &\leq \frac{2\sqrt{2}C_{U,O}^{(1)}}{\gamma_O} \max\{1, \gamma_O\} |xy||Oy|^{\gamma_O-1} + \frac{\pi\sqrt{2}C_{U,O}^{(1)}}{2} |Oy|^{\gamma_O-1} |xy|. \quad \square \end{aligned}$$

We now proceed with geometric bounds for a quadrilateral Q in a ϕ -regular discretization of Σ .

Lemma 3.9. *Let $Q \subset D_O$ be a quadrilateral with vertices w, x, y, z , and let e be any of its four edges. Let z be the vertex of maximum distance to the singularity O . Then,*

$$|e|^2 \leq \frac{2}{\sin^3(\phi)} \text{area}(Q) \quad \text{and} \quad |Oz| \leq \frac{2 + \sin(\phi)}{\sin(\phi)} \max\{|Ow|, |Oy|\}.$$

Proof. If d_1 and d_2 are the two diagonals of Q , and φ_Q is their intersection angle, consider the triangle \triangle formed by e and one of the diagonals, say d_i . While \triangle may lie outside Q , its interior angle opposite to d_i is greater than or equal to an interior angle of Q opposite to d_i . If this angle is greater than $\pi/2$, then $|d_i| \geq |e|$. Otherwise, we can apply the sine theorem and use ϕ -regularity to deduce that:

$$\frac{|e|}{|d_i|} \leq \frac{1}{\sin(\phi)} \Rightarrow |e|^2 \leq \frac{1}{\sin^3(\phi)} |d_1||d_2| \sin(\varphi_Q) = \frac{2}{\sin^3(\phi)} \text{area}(Q).$$

Let us assume that $|Oy| \geq |Ow|$. Using the above result for the diagonal wy and triangle inequality,

$$|Oz| - |Oy| \leq |zy| \leq \frac{|wy|}{\sin(\phi)} \leq \frac{|Ow| + |Oy|}{\sin(\phi)} \leq \frac{2}{\sin(\phi)} |Oy|. \quad \square$$

Lemma 3.10. *Let $Q \subset D_O$ be a quadrilateral with vertices w, x, y, z . Then,*

$$\int_Q |\nabla_Q U_\Lambda|^2 \leq C_{U,O,\phi}^{(6)} \int_Q r^{2\gamma_O-2} r dr d\psi.$$

Proof. Without loss of generality, we assume $|Oy| \geq |Ow|$, and that z has the maximum distance to O . Lemma 3.8 provides bounds for the two discrete difference quotients of U_Λ along the diagonals. By applying Lemma 3.3 together with Lemma 3.9, we obtain the following bound for the discrete gradient:

$$|\nabla_Q U_\Lambda| \leq \frac{2C_{U,O}^{(5)}}{\sin(\phi)} \max\{|Oz|^{\gamma_O-1}, |Oy|^{\gamma_O-1}\} \leq \frac{2C_{U,O}^{(5)}}{\sin(\phi)} \left(\frac{2 + \sin(\phi)}{\sin(\phi)} \right)^{|1-\gamma_O|_0} |Oz|^{\gamma_O-1}.$$

If $\gamma_O \leq 1$, $|Oz|^{\gamma_O-1} \leq r^{\gamma_O-1}$ for all $p = (r, \psi) \in Q$. If $\gamma_O > 1$, we consider the homothety Z of Q with center z and ratio $1/4$. Then, $|Oz| \leq 2r$ for all $p = (r, \psi) \in Z(Q)$, so

$$|Oz|^{2\gamma_O-2} \text{area}(Q) = 16|Oz|^{2\gamma_O-2} \text{area}(Z(Q)) \leq 16 \int_{Z(Q)} (2r)^{2\gamma_O-2} r dr d\psi \leq 2^{2\gamma_O+2} \int_Q r^{2\gamma_O-2} r dr d\psi.$$

In particular,

$$\begin{aligned} \int_Q |\nabla_Q U_\Lambda|^2 &\leq \frac{4 \left(C_{U,O}^{(5)}\right)^2}{\sin^2(\phi)} \left(\frac{2 + \sin(\phi)}{\sin(\phi)}\right)^{2|1-\gamma_O|_0} |Oz|^{2\gamma_O-2} \text{area}(Q) \\ &\leq \frac{4 \left(C_{U,O}^{(5)}\right)^2}{\sin^2(\phi)} \left(\frac{2 + \sin(\phi)}{\sin(\phi)}\right)^{2|1-\gamma_O|_0} 2^{4+2|\gamma_O-1|_0} \int_Q r^{2\gamma_O-2} r dr d\psi. \quad \square \end{aligned}$$

Lemma 3.11. *Let $T = T_{O,h}$ and $T_{(h)} = T_{O,h,(h)}$ be the sets of all quadrilaterals $Q \subset D_O$ of Λ that intersect the disks of radius h and h^{1/γ_O} (if $\gamma_O < 1/2$, otherwise of radius h) around O , respectively. Then, we have the following estimates:*

$$\begin{aligned} \sum_{Q \in T} \int_Q |\nabla U - \nabla_Q U_\Lambda|^2 &\leq C_{U,O,\phi}^{(7)} h^{2\gamma_O} \\ \text{and } \sum_{Q \in T_{(h)}} \int_Q |\nabla U - \nabla_Q U_\Lambda|^2 &\leq C_{U,O,\phi}^{(7,h)} h^2 \quad \text{if } (\Sigma, \Lambda) \text{ is } h\text{-adapted and } \gamma_O \leq 1/2. \end{aligned}$$

Proof. We can see that for any $Q \in T$, it is contained within a disk of radius $3h$ around O . Hence, using Lemmas 3.5 and 3.10, we obtain the following bound:

$$\begin{aligned} \sum_{Q \in T} \int_Q |\nabla U - \nabla_Q U_\Lambda|^2 &\leq \sum_{Q \in T} \int_Q (|\nabla U|^2 + |\nabla_Q U_\Lambda|^2) \leq \left(2 \left(C_{U,O}^{(1)}\right)^2 + C_{U,O,\phi}^{(6)}\right) \int_0^{3h} \int_0^{2\pi/\gamma_O} r^{2\gamma_O-2} r dr d\psi \\ &= 3^{2\gamma_O} \pi \frac{2 \left(C_{U,O}^{(1)}\right)^2 + C_{U,O,\phi}^{(6)}}{\gamma_O^2} h^{2\gamma_O}. \end{aligned}$$

In the case of h -adaptedness, Lemma 3.1 shows that any $Q \in T_{(h)}$ is contained within the disk of radius $\left(3 + \frac{\pi}{\gamma_O}\right) h^{1/\gamma_O}$ around O . Therefore, we obtain a similar bound:

$$\begin{aligned} \sum_{Q \in T_{(h)}} \int_Q |\nabla U - \nabla_Q U_\Lambda|^2 &\leq \left(2 \left(C_{U,O}^{(1)}\right)^2 + C_{U,O,\phi}^{(6)}\right) \int_0^{\left(3 + \frac{\pi}{\gamma_O}\right) h^{1/\gamma_O}} \int_0^{2\pi/\gamma_O} r^{2\gamma_O-2} r dr d\psi \\ &= \left(3 + \frac{\pi}{\gamma_O}\right)^{2\gamma_O} \pi \frac{2 \left(C_{U,O}^{(1)}\right)^2 + C_{U,O,\phi}^{(6)}}{\gamma_O^2} h^2. \quad \square \end{aligned}$$

As observed in Lemma 3.7, the convergence rate depends on the conical singularity of Σ with the smallest singularity index.

Definition. Let $\gamma_\Sigma := \min\{1, \min_{O \in S} \gamma_O\}$ denote the smallest and $\tilde{\gamma}_\Sigma := \max\{1, \max_{O \in S} \gamma_O\}$ the largest singularity index among the conical singularities S of Σ . If there is no conical singularity, then Σ is a torus. For $h > 0$, we denote

$$\lambda_\Sigma(h) := \begin{cases} h & \text{if } \gamma_\Sigma > 1/2, \\ 2h |\log h| & \text{if } \gamma_\Sigma = 1/2, \\ h^{2\gamma_\Sigma} & \text{if } \gamma_\Sigma < 1/2. \end{cases}$$

Now, combining Lemmas 3.7 and 3.11, we can estimate the approximation error in the Second Lemma of Strang, Lemma 3.2.

Proposition 3.12. *If the maximum edge length h of the ϕ -regular discretization (Σ, Λ) satisfies $h \leq C^{(8)}$ or $h \leq C^{(8,h)}$ in the h -adapted case, then*

$$\begin{aligned} \|U - U_\Lambda\|^2 &\leq C_{U,\phi}^{(9)} \lambda_\Sigma(h) \\ \text{and } \|U - U_\Lambda\|^2 &\leq C_{U,\phi}^{(9,h)} h \quad \text{if } (\Sigma, \Lambda) \text{ is } h\text{-adapted.} \end{aligned}$$

Proof. We start by considering a finite cover of Σ with open disks D_O of radius R_O , $O \in \Sigma$, containing no singularities other than possibly O . Let S' denote the set of all O for which D_O is in the above open cover and assume that S' is minimal, i.e., there are no superfluous disks in the cover. Let δ denote the Lebesgue number of the cover and let

$$c := \min \left\{ \frac{\delta}{2}, \left\{ \frac{1}{R_O} \right\}_{O \in S'} \right\}.$$

Next, we define appropriate constants for the different cases of γ_Σ :

- If $\gamma_\Sigma > 1/2$, let $C^{(8)} := \min\{1, c\}$.
- If $\gamma_\Sigma = 1/2$, let $C^{(8)} := \min\{e^{-1/2}, c\}$, where e is Euler's number.
- If $\gamma_\Sigma < 1/2$, we define $K(\Sigma) = 1$ if no singularity O has index $\gamma_O = 1/2$, and otherwise, we choose $K(\Sigma) > 0$ such that $2 \log(t) \leq t^{1-2\gamma_\Sigma}$ for all $t \geq K(\Sigma)$. Then, $C^{(8)} := \min\{K(\Sigma)^{-1}, c\}$.

Clearly, $h \leq R_O$ for all $O \in S'$. For any quadrilateral $Q \in F(\Lambda)$, there is $O \in S'$ such that $Q \subset D_O$ by Lebesgue's number lemma. So Lemmas 3.7 and 3.11 yield the desired estimate:

$$\begin{aligned} \|U - U_\Lambda\|^2 &= \sum_{Q \in F(\Lambda)} \int_Q |\nabla U - \nabla_Q U_\Lambda|^2 \\ &\leq \sum_{O \in S'} \left(\sum_{Q \in T'_{O,h}} \int_Q |\nabla U - \nabla_Q U_\Lambda|^2 + \sum_{Q \in T_{O,h}} \int_Q |\nabla U - \nabla_Q U_\Lambda|^2 \right) \\ &\leq \sum_{O \in S'} \left(C_{U,O,\phi}^{(4)} \lambda_O(h) + C_{U,O,\phi}^{(7)} h^{2\gamma_O} \right) \\ &\leq \sum_{O \in S'} \left(C_{U,O,\phi}^{(4)} + C_{U,O,\phi}^{(7)} \right) \cdot \begin{cases} h & \text{if } \gamma_\Sigma > 1/2, \\ 2h |\log h| & \text{if } \gamma_\Sigma = 1/2, \\ h^{2\gamma_\Sigma} & \text{if } \gamma_\Sigma < 1/2. \end{cases} \end{aligned}$$

To arrive at the last line, we used the following: Since $0 < h \leq 1$, h^x is a decreasing function in x . If $h \leq e^{-1/2}$, then $h^x \leq h \leq 2h |\log h|$ for all $x \geq 1$. Due to $h \leq R_O^{\pm 1}$, $h |\log h R_O^{-1}| \leq h |\log h| + h |\log R_O| \leq 2h |\log h|$. By construction, if $\gamma_\Sigma < 1/2$ and $\gamma_O = 1/2$, $\lambda_O(h) \leq 2h |\log h| \leq h^{2\gamma_\Sigma}$ if $h \leq C^{(8)}$.

In the h -adapted case, the proof follows similarly, with $C^{(8,h)} := \min\{1, c\}$. \square

Remark. ϕ -regularity around conical singularities is essential for the convergence of the Dirichlet energies in Proposition 3.12 if there is a conical singularity with $\gamma_O < 1/2$. We illustrate this with an example adapted from Bobenko and Skopenkov's work on triangular decompositions [9] to our setting, where we need to bound the interior angles of quadrilaterals as well as the intersection angles of diagonals.

Let $\gamma_O < 1/2$ and $k > 1/(1 - 2\gamma_O)$. Consider the harmonic function $U(r, \psi) := r^{\gamma_O} \cos(\gamma_O \psi)$ in D_O . It has bounded Dirichlet energy in this domain.

First, let Q be the rhombus with black vertices O and $(h^k, 0)$ such that the white diagonal has length h . The edges of Q have length $\sqrt{h^2 + h^{2k}}/2 < \sqrt{2}h/2 < h$ if $h < 1$. U takes identical values on the two white vertices. Thus, $\nabla_Q U_\Lambda = h^{k(\gamma_0-1)}$. The area of Q is $h^{k+1}/2$. Hence, $2 \int_Q |\nabla_Q U_\Lambda|^2 = h^{2k(\gamma_0-1)+k+1}$. Since $2k(\gamma_0 - 1) + k + 1 = 1 - k(1 - 2\gamma_0) < 0$, the discrete Dirichlet energy of U_Λ diverges to infinity as $h \rightarrow 0$. Note that the interior angle of Q at O goes to zero as $h \rightarrow 0$.

Second, let Q be the rectangle with one black vertex b_- at O and its two white vertices w_- and w_+ being at $(h^k, 0)$ and $(h, \pi/2)$, respectively. The edges of Q have length h and $h^k < h$ if $h < 1$. As $h \rightarrow 0$, the intersection angle of the black and the white diagonal approaches zero. We can bound the length of $\nabla_Q U_\Lambda$ from below by considering the discrete difference quotient of U_Λ between $(b_- + w_+)/2$ and $(b_+ + w_-)/2$. This leads to the inequality

$$\begin{aligned} |\nabla_Q U_\Lambda| &\geq \frac{\left(\sqrt{h^2 + h^{2k}}\right)^{\gamma_0} \cos(\gamma_0 \angle w_- b_- b_+) + h^{k\gamma_0} - h^{\gamma_0} \cos(\gamma_0 \pi/2)}{2h^k} \\ &> \frac{h^{\gamma_0-k}}{2} \left(\left(1 + h^{2(k-1)}\right)^{\gamma_0/2} \cos(\pi/4) + h^{(k-1)\gamma_0} - \cos(\pi/4) \right) \\ &> \frac{h^{\gamma_0-k}}{2\sqrt{2}} \left(\left(1 + h^{2(k-1)}\right)^{\gamma_0/2} - 1 + h^{(k-1)\gamma_0} \right) > \frac{h^{k(\gamma_0-1)}}{2\sqrt{2}}. \end{aligned}$$

The area of the rectangle is h^{1+k} , which leads to $8 \int_Q |\nabla_Q U_\Lambda|^2 > h^{2k(\gamma_0-1)+k+1} \rightarrow \infty$ as $h \rightarrow 0$.

3.4 The consistency error

Now let us bound the consistency error in Lemma 3.2. We want to estimate $|a(U, f)|$ for an arbitrary function $f : V(\Lambda) \rightarrow \mathbb{R}$.

The function f induces a corresponding function $f : V(X) \rightarrow \mathbb{R}$ on the vertices of the medial graph by taking the arithmetic mean: If $e = bw$ is an edge of Λ and we identify e with its midpoint, then $f(e) := (f(b) + f(w))/2$. On the Varignon parallelogram $F_Q \subset \Sigma$ associated with a quadrilateral $Q \in F(\Lambda)$, we can linearly interpolate f . We extend this interpolation to the entire $Q \subset \Sigma$. Doing this for all quadrilaterals $Q \in F(\Lambda)$ gives us a well-defined function in $L^2(\Sigma)$, which we also denote as f . By construction, we can choose a representative of f that is continuous at midpoints of edges (i.e., at vertices of X), where it agrees with the original function $f : V(X) \rightarrow \mathbb{R}$. Similarly, $U_\Lambda \in L^2(\Sigma)$ is defined as a piecewise linear function that is continuous along midpoints of edges. On a given quadrilateral Q , we always consider f and U_Λ to be continuous also at the boundary. This means, in particular, that we consider generally different representatives of $f, U_\Lambda \in L^2(\Sigma)$ on the single quadrilaterals.

Functions $f \in L^2(\Sigma)$ are analogous to the *Crouzeix-Raviart elements* used for quadrilaterals. The Crouzeix-Raviart elements are introduced by Braess in [10] as the simplest nonconforming elements for discretizing the Poisson problem. The term *nonconforming* indicates that the discrete functions are not continuous, unlike the *conforming* elements, which are continuous and piecewise linear. The conforming elements correspond to the linear interpolations of f and u on triangles, as considered by Bobenko and Skopenkov in [9].

To bound $|a(U, f)|$, we adopt the ideas from Braess [10] for the Crouzeix-Raviart elements on a planar triangulation and adapt them to our setting. Let $T_{O,h}$ be the set of all quadrilaterals $Q \subset D_O$ of Λ that intersect the disk of radius h around the conical singularity O . We define \tilde{T} as the complement of $\bigcup_{O \in S} T_{O,h}$ in $F(Q)$.

Though ∇U and $\nabla_Q f$ depend on the chosen chart, their scalar product and lengths are chart-independent, as any two (discrete) charts differ by an isometry. Therefore, we can work with these expressions without specifying the chart.

To estimate the consistency error in Lemma 3.2, we use Green's first identity, denoting by n the outer

unit normal vector on the edges of the quadrilateral Q :

$$\int_Q \nabla U \cdot \nabla_Q f = \int_{\partial Q} (\partial_n U) f - \int_Q \Delta u f = \sum_{e \in \partial Q} \int_e f \partial_n u$$

since U is harmonic. The normal derivative $\partial_n U$ is chart-independent and well-defined on the edges of a quadrilateral Q . However, it changes sign on the same edge when considering the other quadrilateral Q' sharing e . Thus, the sum of the expressions $\int_e f(e) \partial_n U$ corresponding to the two quadrilaterals sharing the edge e cancels out. Hence,

$$\begin{aligned} a(U, f) &= \sum_{Q \in \mathcal{F}(\Lambda)} \int_Q \nabla U \cdot \nabla_Q f \\ &= \sum_{O \in S} \sum_{Q \in T_{O,h}} \int_Q \nabla U \cdot \nabla_Q f - \sum_{O \in S} \sum_{Q \in T_{O,h}} \sum_{e \in \partial Q} \int_e f(e) \partial_n U + \sum_{Q \in \tilde{T}} \sum_{e \in \partial Q} \int_e (f - f(e)) \partial_n U. \quad (\star) \end{aligned}$$

Now we focus on the last term. Since f is linear on Q , it is also linear on the edge $e \subset Q$, and thus $\int_e (f - f(e)) = 0$ because it is zero at the midpoint of e . We can subtract a constant from $\partial_n U$ for each oriented edge without changing the sum's value. We choose to subtract $\partial_n U_\Lambda$.

$$\begin{aligned} \left| \sum_{Q \in \tilde{T}} \sum_{e \in \partial Q} (f - f(e)) \partial_n U \right| &\leq \sum_{Q \in \tilde{T}} \sum_{e \in \partial Q} \int_e |(f - f(e)) \partial_n (U - U_\Lambda)| \\ &\leq \sum_{Q \in \tilde{T}} \sum_{e \in \partial Q} \sqrt{\int_e (f - f(e))^2} \sqrt{\int_e (\partial_n (U - U_\Lambda))^2} \\ &\leq \sum_{Q \in \tilde{T}} \sum_{e \in \partial Q} \sqrt{2 \int_0^{|e|/2} \left| \nabla_Q f \cdot \frac{e}{|e|} \right|^2 s^2 ds} \sqrt{\int_e |\nabla (U - U_\Lambda)|^2} \\ &\leq \sum_{Q \in \tilde{T}} \sum_{e \in \partial Q} \sqrt{\frac{|\nabla_Q f|^2 |e|^2}{12}} \sqrt{|e| \int_e |\nabla (U - U_\Lambda)|^2} \\ &\leq \sqrt{\sum_{Q \in \tilde{T}} \sum_{e \in \partial Q} \frac{|\nabla_Q f|^2 |e|^2}{12}} \sqrt{\sum_{Q \in \tilde{T}} \sum_{e \in \partial Q} |e| \int_e |\nabla (U - U_\Lambda)|^2} \\ &\leq \sqrt{\sum_{Q \in \tilde{T}} \frac{2 |\nabla_Q f|^2 \text{area}(Q)}{3 \sin^3 \phi}} \sqrt{\sum_{Q \in \tilde{T}} \sum_{e \in \partial Q} |e| \int_e |\nabla (U - U_\Lambda)|^2} \\ &= \sqrt{\frac{2}{3 \sin^3 \phi}} \|f\|_{\tilde{T}} \sqrt{\sum_{Q \in \tilde{T}} \sum_{e \in \partial Q} |e| \int_e |\nabla (U - U_\Lambda)|^2} \end{aligned}$$

by Cauchy-Schwarz inequality and the geometric bound in Lemma 3.9. Here, $|e|$ is the length of edge e , and $\|f\|_{\tilde{T}}^2 := \sum_{Q \in \tilde{T}} |\nabla_Q f|^2 \text{area}(Q)$. In the case of h -adapted discrete Riemann surfaces, replace the sets $T_{O,h}$ by the sets $T_{O,h,(h)}$ corresponding to the radius h^{1/γ_O} if $\gamma_O < 1/2$.

In the next step, we proceed to bound the consistency error, following a similar approach as in the previous Section 3.3. In the following, we focus on a conical singularity $O \in \Sigma$ and the corresponding chart (D_O, g_O) , where D_O is a disk with radius R_O . We start by establishing the analogue of Lemmas 3.6.

Lemma 3.13. *For a quadrilateral $Q \subset D_O$ that does not intersect the disk of radius h around O , we have the following bound:*

$$\sum_{e \in \partial Q} |e| \int_e |\nabla U - \nabla_Q U_\Lambda|^2 \leq \frac{8C_{U,O,\phi}^{(3)}}{\sin^3 \phi} h \int_Q r^{2\gamma_O - 2} dr d\psi.$$

Proof. We make use of the geometric bound from Lemma 3.9. Specifically, we have:

$$\sum_{e \in \partial Q} |e| \int_e |\nabla U - \nabla_Q U_\Lambda|^2 \leq \sum_{e \in \partial Q} |e|^2 \max_{w \in Q} |\nabla U(w) - \nabla_Q U_\Lambda|^2 \leq \frac{8}{\sin^3 \phi} \text{area}(Q) \max_{w \in Q} |\nabla U(w) - \nabla_Q U_\Lambda|^2.$$

Up to the constant factor, this expression is precisely the same one we bounded in Lemma 3.6. \square

Using Lemma 3.13, we prove the following lemma in exactly the same way as Lemma 3.7.

Lemma 3.14. *Let $T' = T'_{O,h}$ and $T'_{(h)} = T'_{O,h,(h)}$ be the sets of all quadrilaterals $Q \subset D_O$ of Λ that do not intersect the disks of radius h and h^{1/γ_O} (if $\gamma_O < 1/2$, otherwise of radius h) around O , respectively. Additionally, we assume $h \leq R_O$. Then,*

$$\sum_{Q \in T'} \sum_{e \in \partial Q} |e| \int_e |\nabla u - \nabla_Q u_\Lambda|^2 \leq \frac{8C_{U,O,\phi}^{(4)}}{\sin^3 \phi} \lambda_O(h)$$

and $\sum_{Q \in T'_{(h)}} \sum_{e \in \partial Q} |e| \int_e |\nabla u - \nabla_Q u_\Lambda|^2 \leq \frac{8C_{U,O,\phi}^{(4,h)}}{\sin^3 \phi} h$ if (Σ, Λ) is h -adapted and $\gamma_O \leq 1/2$.

We can then derive the following corollary, which is shown in a similar way as Proposition 3.12.

Corollary 3.15.

$$\sum_{Q \in \tilde{T}} \sum_{e \in \partial Q} |e| \int_e |\nabla(U - U_\Lambda)|^2 \leq \frac{8}{\sin^3 \phi} \lambda_\Sigma(h) \left(\sum_{O \in S} C_{U,O,\phi}^{(4)} \right) \quad \text{if } h \leq C^{(8)}$$

and $\sum_{Q \in \tilde{T}} \sum_{e \in \partial Q} |e| \int_e |\nabla(U - U_\Lambda)|^2 \leq \frac{8}{\sin^3 \phi} h \left(\sum_{O \in S} C_{U,O,\phi}^{(4,h)} \right)$ if (Σ, Λ) is h -adapted and $h \leq C^{(8,h)}$.

Here, we define $C_{U,O,\phi}^{(4,h)} := C_{U,O,\phi}^{(4)}$ if $\gamma_O \geq 1/2$.

Now, let us focus on the contribution of $Q \in T_{O,h}$, where $O \in S$. We define $\|f\|_{T_{O,h}}^2 := \sum_{Q \in T_{O,h}} \int_Q |\nabla_Q f|^2$ and $\|f\|_S^2 := \sum_{O \in S} \|f\|_{T_{O,h}}^2$.

Lemma 3.16.

$$\left| \sum_{O \in S} \sum_{Q \in T_{O,h}} \int_Q \nabla U \cdot \nabla_Q f \right| \leq C_{U,\phi}^{(10)} \sqrt{\lambda_\Sigma(h)} \|f\|_S \quad \text{if } h \leq C^{(8)}$$

and $\left| \sum_{O \in S} \sum_{Q \in T_{O,h,(h)}} \int_Q \nabla U \cdot \nabla_Q f \right| \leq C_{U,\phi}^{(10,h)} h \|f\|_S$ if (Σ, Λ) is h -adapted and $h \leq C^{(8,h)}$.

Proof. First, observe that any $Q \in T_{O,h}$ is contained in the disk of radius $3h$ around O . Using Cauchy-Schwarz inequality and Lemma 3.5, we have:

$$\begin{aligned} \left| \sum_{Q \in T_{O,h}} \int_Q \nabla U \cdot \nabla_Q f \right| &\leq \sum_{Q \in T_{O,h}} \sqrt{\int_Q |\nabla U|^2} \sqrt{\int_Q |\nabla_Q f|^2} \\ &\leq \sqrt{\sum_{Q \in T_{O,h}} \int_Q |\nabla U|^2} \sqrt{\sum_{Q \in T_{O,h}} \int_Q |\nabla_Q f|^2} \\ &\leq \|f\|_{T_{O,h}} \sqrt{2} C_{U,O}^{(1)} \sqrt{\int_0^{3h} \int_0^{2\pi/\gamma_O} r^{2\gamma_O-2} r dr d\psi} = 3^{\gamma_O} \sqrt{2\pi} \frac{C_{U,O}^{(1)}}{\gamma_O} h^{\gamma_O} \|f\|_{T_{O,h}}. \end{aligned}$$

The results now follow from the inequality of the arithmetic and the quadratic mean for the $\|f\|_{T_{O,h}}$ and $h \leq C^{(8)}$ in a similar way as in the proof of Proposition 3.12. The h -adapted case follows similarly. \square

Lemma 3.17.

$$\left| \sum_{O \in S} \sum_{Q \in T_{O,h}} \sum_{e \in \partial Q} \int_e f(e) \partial_n U \right| \leq C_{U,\phi}^{(11)} \sqrt{\lambda_\Sigma(h)} \|f\|_S \quad \text{if } h \leq C^{(8)}$$

and $\left| \sum_{O \in S} \sum_{Q \in T_{O,h,(h)}} \sum_{e \in \partial Q} \int_e f(e) \partial_n U \right| \leq C_{U,\phi}^{(11,h)} h \|f\|_S \quad \text{if } (\Sigma, \Lambda) \text{ is } h\text{-adapted and } h \leq C^{(8,h)}.$

Proof. Let $Q \subset D_O$ be a quadrilateral with vertices w, x, y, z . Since U is harmonic, $\sum_{e \in \partial Q} \int_e \partial_n U = 0$ follows from Green's first identity. In particular, we can add a constant to all $f(e)$ without changing $\sum_{e \in \partial Q} \int_e f(e) \partial_n U = 0$. We choose this constant to be $(f(w) + f(x) + f(y) + f(z))/4$. Then, the four values of f on the four edges become $\pm((f(z) - f(x)) \pm (f(y) - f(w)))/4$. Their absolute value can be bounded from above by:

$$|\nabla_Q f| \frac{|d_1| + |d_2|}{4} \leq |\nabla_Q f| \frac{\sqrt{|d_1||d_2|}}{2} \leq |\nabla_Q f| \frac{\sqrt{\text{area}(Q)}}{\sqrt{2} \sin(\phi)}$$

using ϕ -regularity of Q . Here, d_1, d_2 denote the two diagonals of Q .

Without loss of generality, assume z is the vertex of maximum distance to O . Since $|\partial_n U| \leq |\nabla U|$, we can use the same constant $C^{(5)}U, O$ and the same ideas as in Lemma 3.8 to bound $\sum_{e \in \partial Q} \int_e |\partial_n U|$ by:

$$C_{U,O}^{(5)} (|yz||Oz|^{\gamma_O-1} + |zw||Oz|^{\gamma_O-1} + |wx| \max\{|Ow|, |Ox|\}^{\gamma_O-1} + |xy| \max\{|Ox|, |Oy|\}^{\gamma_O-1}).$$

Let p, p' be two adjacent vertices among w, x, y . Assume $|Op| \geq |Op'|$. By triangle inequality,

$$|Oz| - |Op| \leq |pz| = \frac{|pz|}{|pp'|} |pp'| \leq \frac{|pz|}{|pp'|} (|Op| + |Op'|) \leq 2 \frac{|pz|}{|pp'|} |Op| \Rightarrow |Oz| \leq \left(1 + 2 \frac{|pz|}{|pp'|}\right) |Op|.$$

Together with the bound of edge lengths in Lemma 3.9 (which also bounds half the length of a diagonal), we now deduce:

$$|pp'| |Op|^{\gamma_O-1} \leq |pp'|^{\gamma_O} |pp'|^{1-\gamma_O} \left(1 + 2 \frac{|pz|}{|pp'|}\right)^{1-\gamma_O|0|} \leq \sqrt{\frac{2}{\sin^3(\phi)} \text{area}(Q)} 5^{1-\gamma_O|0|} |Oz|^{\gamma_O-1}.$$

We thus obtain:

$$\sum_{e \in \partial Q} \int_e |\partial_n U| \leq 2C_{U,O}^{(5)} \left(1 + 5^{1-\gamma_O|0|}\right) \sqrt{\frac{2}{\sin^3(\phi)} \text{area}(Q)} |Oz|^{\gamma_O-1}.$$

In the following, we denote by z_Q the vertex of the quadrilateral Q that has the maximum distance to O . Combining the above two results and applying the Cauchy-Schwarz inequality again yields:

$$\begin{aligned} \left| \sum_{Q \in T_{O,h}} \sum_{e \in \partial Q} \int_e f(e) \partial_n U \right| &\leq \sum_{Q \in T_{O,h}} \frac{2C_{U,O}^{(5)} (1 + 5^{1-\gamma_O|0|})}{\sin^2(\phi)} |\nabla_Q f| |Oz_Q|^{\gamma_O-1} \text{area}(Q) \\ &\leq \frac{2C_{U,O}^{(5)} (1 + 5^{1-\gamma_O|0|})}{\sin^2(\phi)} \sqrt{\sum_{Q \in T_{O,h}} |\nabla_Q f|^2 \text{area}(Q)} \sqrt{\sum_{Q \in T_{O,h}} |Oz_Q|^{2\gamma_O-2} \text{area}(Q)} \\ &\leq \frac{2C_{U,O}^{(5)} (1 + 5^{1-\gamma_O|0|})}{\sin^2(\phi)} \|f\|_{T_{O,h}} \sqrt{\sum_{Q \in T_{O,h}} |Oz_Q|^{2\gamma_O-2} \text{area}(Q)}. \end{aligned}$$

Introducing polar coordinates (r, ψ) around O again, we can use for the latter term the results that we obtained in the proofs of Lemmas 3.10 and 3.11. Thus,

$$\sum_{Q \in T_{O,h}} |Oz_Q|^{2\gamma_O-2} \text{area}(Q) \leq 2^{4+2|\gamma_O-1|_0} \sum_{Q \in T_{O,h}} \int_Q r^{2\gamma_O-2} r dr d\psi \leq 2^{4+2|\gamma_O-1|_0} \frac{3^{2\gamma_O} \pi}{\gamma_O^2} h^{2\gamma_O}.$$

The results now follow from the inequality of the arithmetic and the quadratic mean for the $\|f\|_{T_{O,h}}$ and $h \leq C^{(8)}$ in a similar way as in the proof of Proposition 3.12. The h -adapted case follows similarly. \square

By applying Corollary 3.15, Lemma 3.16, and Lemma 3.16, we can bound the three sums in Equation (\star) , leading to an estimate for the consistency error in Lemma 3.2.

Proposition 3.18. *For a given function $f : V(\Lambda) \rightarrow \mathbb{R}$, if the maximum edge length h of the ϕ -regular discretization (Σ, Λ) satisfies $h \leq C^{(8)}$ or $h \leq C^{(8,h)}$ in the h -adapted case, then the consistency error can be bounded as follows:*

$$a(u, f) \leq C_{U,\phi}^{(12)} \sqrt{\lambda_\Sigma(h)} \|f\|$$

and $a(u, f) \leq C_{U,\phi}^{(12,h)} \sqrt{h} \|f\|$ in the h -adapted case.

3.5 The convergence theorems

We now present the convergence theorem that summarizes the results from the previous two sections. This theorem is analogous to Lemma 4.16 in [9], adapted to our context.

Theorem 3.19. *Let $P \in \mathbb{R}^{2g}$ be a given vector of periods. Consider Ω , the unique smooth holomorphic differential with real parts of its a - and b -periods given by P , and ω , the unique discrete holomorphic differential with real parts of its black and white a - and b -periods given by P , such that corresponding black and white a - and b -periods coincide. Let $U := \int \text{Re}(\Omega)$ and $u := \int \text{Re}(\omega)$ be the corresponding multi-valued (discrete) harmonic functions.*

For any ϕ -regular discretization (Σ, Λ) with a maximal side length h , the following holds:

$$\frac{1}{2} |\langle \Omega, \Omega \rangle - \langle \omega, \omega \rangle| = \left| \|U\|^2 - \|u\|^2 \right| \leq C_{P,\phi}^{(13)} \lambda_\Sigma(h) \quad \text{if } h \leq C^{(8)}$$

and $\frac{1}{2} |\langle \Omega, \Omega \rangle - \langle \omega, \omega \rangle| = \left| \|U\|^2 - \|u\|^2 \right| \leq C_{P,\phi}^{(13,h)} h \quad \text{if } (\Sigma, \Lambda) \text{ is } h\text{-adapted and } h \leq C^{(8,h)}.$

Proof. By applying the Second Lemma of Strang, Lemma 3.2, along with the estimates on the approximation and consistency errors in Propositions 3.12 and 3.18, we deduce the inequality

$$\|U - u\| \leq 2 \inf_{v \in M_P} \|U - v\| + \sup_{f \in M_0} \frac{|a(U, f)|}{\|f\|} \leq 2\sqrt{C_{U,\phi}^{(9)} \lambda_\Sigma(h)} + C_{U,\phi}^{(12)} \sqrt{\lambda_\Sigma(h)}.$$

Now, using the Cauchy-Schwarz inequality for the positive definite scalar product a , we have

$$\begin{aligned} \left| \|U\|^2 - \|u\|^2 \right| &= |a(U - u, U + u)| = |a(U - u, U - u) + 2a(U - u, U)| \\ &\leq \|U - u\|^2 + 2|a(U - u, U)| \leq \|U - u\|^2 + 2\|U - u\| \|U\| \\ &\leq \left(2\sqrt{C_{U,\phi}^{(9)}} + C_{U,\phi}^{(12)} \right)^2 \lambda_\Sigma(h) + 2 \left(2\sqrt{C_{U,\phi}^{(9)}} + C_{U,\phi}^{(12)} \right) \|U\| \sqrt{\lambda_\Sigma(h)} \\ &\leq \left(4 \left(C_{U,\phi}^{(9)} + \sqrt{C_{U,\phi}^{(9)}} \|U\| \right) + (C_{U,\phi}^{(12)})^2 + 2\|U\| C_{U,\phi}^{(12)} \right) \lambda_\Sigma(h) \end{aligned}$$

since $h \leq C^{(8)} \leq 1$. The argument for h -adapted discrete Riemann surfaces follows similarly. \square

The following corollary, which will be useful in Section 4 when we establish the boundedness of the discrete energy form E_Λ , is presented:

Corollary 3.20. *Let $P^B, P^W \in \mathbb{R}^{2g}$ be two given vectors of periods. Let ω' be the unique discrete holomorphic differential with the real parts of its black and white a - and b -periods given by P^B and P^W , respectively. Let $u' := \int \operatorname{Re}(\omega')$ be the corresponding multi-valued discrete harmonic function. Then, $\frac{1}{2}\langle \omega', \omega' \rangle = |u'|^2 \leq C_{P^B, P^W, \phi}^{(14)}$ holds true for any ϕ -regular discretization (Σ, Λ) that satisfies $h \leq C^{(8)}$.*

Proof. We define multi-valued harmonic functions U^B and U^W with periods P^B and P^W , respectively. Restricting them to $V(\tilde{\Lambda})$, we denote these restrictions as U_Λ^B and U_Λ^W . We then introduce the discrete function $U^{B,W} : V(\tilde{\Lambda}) \rightarrow \mathbb{R}$, which agrees with U^B on black vertices and with U_Λ^W on white vertices.

As u' is a discrete harmonic function, and $U_\Lambda^{B,W}$ shares the same periods, we have $|u'|^2 \leq |U_\Lambda^{B,W}|^2$ by Corollary 2.2. In a chart z_Q of a given quadrilateral $Q \in F(\Lambda)$, let's denote b and $w \in \mathbb{C}$ as unit vectors parallel to the black and white diagonal, respectively. Due to the construction, we find that $\langle \nabla_Q U^{B,W}, b \rangle = \langle \nabla_Q U^B, b \rangle$ and $\langle \nabla_Q U^{B,W}, w \rangle = \langle \nabla_Q U^W, w \rangle$. Therefore, we can bound $|\nabla_Q U_\Lambda^{B,W}|^2$ as follows:

$$|\nabla_Q U_\Lambda^{B,W}|^2 \leq \frac{4}{\sin^2 \phi} \max \{ (\nabla_Q U^B \cdot b)^2, (\nabla_Q U^W \cdot w)^2 \} \leq \frac{4}{\sin^2 \phi} (|\nabla_Q U^B|^2 + |\nabla_Q U^W|^2)$$

due to Lemma 3.3. By integrating over Σ and using Theorem 3.19, we obtain the inequality:

$$\begin{aligned} \|u'\|^2 &\leq \|U_\Lambda^{B,W}\|^2 \leq \frac{4}{\sin^2 \phi} (\|U_\Lambda^B\|^2 + \|U_\Lambda^W\|^2) \leq \frac{4}{\sin^2 \phi} (\|U^B\|^2 + \|U^B - U_\Lambda^B\|^2 + \|U^W\|^2 + \|U^W - U_\Lambda^W\|^2) \\ &\leq \frac{4}{\sin^2 \phi} (\|U^B\|^2 + \|U^W\|^2 + C_{P^B, \phi}^{(13)} + C_{P^W, \phi}^{(13)}) =: C_{P^B, P^W, \phi}^{(14)}. \end{aligned} \quad \square$$

Now we introduce some necessary notions to define the convergence of the discrete Dirichlet energy to its smooth counterpart as quadratic forms.

Definition. Let $M = (M_{ij})_{i,j=1}^k$ be a real $k \times k$ -matrix. We denote the Frobenius norm of M by

$$\|M\| := \sqrt{\sum_{i,j=1}^k M_{ij}^2}.$$

Remark. The Frobenius norm is sub-multiplicative, $\|MN\| \leq \|M\| \cdot \|N\|$, for any two real $k \times k$ -matrices M, N . If M is a real number, then $\|M\| = |M|$.

Definition. For a discretization (Σ, Λ) of the Riemann surface Σ , we denote by h the maximal edge length of the embedded quad-graph Λ . Let X_Λ be a square matrix depending on the discretization (Σ, Λ) (including dependency on Σ), and X_Σ a matrix of the same size depending solely on the geometry of Σ . We write $X_\Lambda \rightarrow X_\Sigma$ as $h \rightarrow 0$ if there exist two constants c and C , depending only on Σ and the angle parameter ϕ , such that $\|X_\Lambda - X_\Sigma\| \leq C\lambda_\Sigma(h)$ holds true for any ϕ -regular discretization (Σ, Λ) satisfying $h \leq c$. In the case of h -adapted discretizations, we replace $\lambda_\Sigma(h)$ with h .

The convergence of energies in Theorem 3.19 implies the convergence of the quadratic forms.

Theorem 3.21. *If the maximal edge length of a sequence of ϕ -regular discrete Riemann surfaces on Σ approaches zero, then the quadratic form corresponding to the Dirichlet energy of discrete harmonic forms with equal black and white periods converges to its smooth counterpart, $E_\Lambda^{B=W} \rightarrow E_\Sigma$ as $h \rightarrow 0$.*

Proof. Theorem 3.19 ensures that for any given vector $P \in \mathbb{R}^{2g}$,

$$|P^T E_\Lambda^{B=W} P - P^T E_\Sigma P| = 2|\langle U, U \rangle - \langle u, u \rangle| \leq C_{P, \phi}^{(13)} \lambda_\Sigma(h)$$

for all discretizations (Σ, Λ) with maximum edge length $h \leq C^{(8)}$. Here, U and u are the corresponding multi-valued smooth and discrete harmonic functions with periods given by P . The dependency of $C_{P,\phi}^{(13)}$ on P corresponds to the dependency on $\|U\|$ and $\max_{z \in \overline{g_O(D_O)}} \|D^k U_O(z)\|$ for $k = 1, 2$ and charts (D_O, g_O) , $O \in S'$, used in the proof of Proposition 3.12. As U depends smoothly on P , $C_{P,\phi}^{(13)}$ depends continuously on P , and we denote $C_\phi^{(15)} := \max_{|P|=1} C_P$. It follows that

$$|P^T(E_\Lambda^{B=W} - E_\Sigma)P| \leq C_\phi^{(15)} \lambda_\Sigma(h) \|P\|^2$$

for all $P \in \mathbb{R}^{2g}$ provided that $h \leq C^{(8)}$. Finally, we show that $|E_\Lambda^{B=W} - E_\Sigma| \leq \sqrt{2g} C_\phi^{(15)} \lambda_\Sigma(h)$ by observing that the difference is diagonalizable, and the absolute value of any eigenvalue is bounded by $C_\phi^{(15)} \lambda_\Sigma(h)$. The h -adapted case is treated similarly. \square

In conclusion, we examine the convergence of multi-valued discrete holomorphic functions in the context of nondegenerate uniform sequences of orthodiagonal discrete Riemann surfaces (Σ, Λ_n) . This convergence mirrors the result presented in Theorem 5.3 by Bobenko and Skopenkov [9]. Their proof relies on a similar statement established by Skopenkov in [32] for planar orthodiagonal quadrilateral lattices. The key transformation of a Delaunay triangulation into a Delaunay-Voronoi quadrangulation, discussed in [9, 32], plays a pivotal role in the argument. Furthermore, the adaptations made to handle conical singularities in [9] naturally extend to the quadrilateral case.

In light of these connections and to avoid redundancy, we opt not to reproduce the proof of the theorem here. For interested readers seeking a detailed proof, we refer them to the upcoming master's thesis of Maximilian Pschigode (Technische Universität Berlin).

Definition. We introduce the notion of a *nondegenerate uniform sequence* of discrete Riemann surfaces (Σ, Λ_n) , assuming an atlas $(D_O, g_O)_{O \in S}$ of Σ and an angle parameter $\phi > 0$. To be classified as *nondegenerate uniform*, the sequence must satisfy two conditions:

- The discrete Riemann surfaces (Σ, Λ_n) must be ϕ -regular.
- For any point p that does not lie within any D_O associated with a singularity $O \in S$, the number of vertices in $V(\Lambda_n)$ within any disk centered at p and having a radius equal to the maximal edge length must be less than a fixed constant C that is independent of n . If p does lie within a D_O for some $O \in S$, the same condition should apply, or alternatively, the number of vertices $g_O(V(\Lambda_n \cap D_O))$ within any disk centered at $g_O(p)$ and having a radius equal to the maximal edge length should be smaller than C .

It is worth noting that the boundedness of the interior angles of the quadrilaterals implies a bounded ratio of the lengths of their diagonals, which is the condition effectively used in [32]. The modification of the second condition for points close to a conical singularity arises from the h -adapted case and was introduced by Bobenko and Bücking in [4].

Theorem 3.22. *Let (Σ, Λ_n) be a sequence of nondegenerate uniform orthodiagonal discrete Riemann surfaces, such that the maximal edge length converges to zero as n tends to infinity. Consider $P_n \in \mathbb{R}^{2g}$, a sequence of vectors converging to a vector P . Let $(p_n, p'_n) \in E(\Lambda_n)$ be a sequence of edges such that $p_n \rightarrow p \in \Sigma$ as $n \rightarrow \infty$.*

Let $U : \tilde{\Sigma} \rightarrow \mathbb{R}$ be the unique multi-valued harmonic function with periods given by P , satisfying $U(p) = 0$. Let $u_n : V(\tilde{\Lambda}_n) \rightarrow \mathbb{R}$ be the unique real multi-valued discrete harmonic function with equal black and white periods given by P_n , satisfying $u_n(p_n) = u_n(p'_n) = 0$.

Then, the functions u_n converge to U uniformly on each compact subset of $\tilde{\Sigma}$ as n approaches infinity.

4 Convergence of the discrete period matrix

Before delving into the convergence of discrete period matrices to their smooth counterpart in Theorem 4.3, we shall first introduce two lemmas that will be essential for the proof.

Lemma 4.1. Let $M := \begin{pmatrix} A & B \\ B^T & C \end{pmatrix}$ be a symmetric and positive definite $2g \times 2g$ -matrix with the $g \times g$ -

blocks $A = A^T, B, C = C^T$. Consider the $g \times 2g$ -matrix $L := (1_g \ 1_g)$ consisting of twice the identity matrix.

Then, the matrix $LML^T - 4(LM^{-1}L^T)^{-1}$ is positive semidefinite. Moreover, if this matrix approaches zero and M remains bounded throughout the convergence, then $A - C$ and $B - B^T$ also approach zero.

We would like to express our gratitude to Günter Rote for providing us with the proof of positive semidefiniteness.

Proof. Let $J := \frac{1}{\sqrt{2}} \begin{pmatrix} 1_g & 1_g \\ 1_g & -1_g \end{pmatrix}$, which is an orthogonal and symmetric matrix ($J^{-1} = J^T = J$). We

define $K := (1_g \ 0_g)$, a $g \times 2g$ -matrix with the identity matrix and the zero matrix.

By performing some algebraic manipulations, we obtain:

$$LML^T - 4(LM^{-1}L^T)^{-1} = 2KJMJK^T - 4(2KJM^{-1}JK^T)^{-1} = 2K\hat{M}K^T - 2(K\hat{M}^{-1}K^T)^{-1},$$

where $\hat{M} := JMJ$. Since M is positive definite, $\hat{M} := \begin{pmatrix} \hat{A} & \hat{B} \\ \hat{B}^T & \hat{C} \end{pmatrix}$ is also positive definite. Specifically,

the upper left block of \hat{M}^{-1} is given by the inverse of the Schur complement $\hat{M}/\hat{C} = \hat{A} - \hat{B}^T\hat{C}^{-1}\hat{B}$, and thus $K\hat{M}^{-1}K^T = (\hat{A} - \hat{B}^T\hat{C}^{-1}\hat{B})^{-1}$. This simplifies the expression to:

$$LML^T - 4(LM^{-1}L^T)^{-1} = 2\hat{A} - 2(\hat{A} - \hat{B}^T\hat{C}^{-1}\hat{B}) = 2\hat{B}^T\hat{C}^{-1}\hat{B}.$$

Since \hat{M} and its positive definite diagonal block \hat{C} remain bounded during convergence, we know that \hat{C}^{-1} is also bounded away from zero. Thus, $\hat{B}^T\hat{C}^{-1}\hat{B}$ is positive semidefinite.

By setting Q as an orthogonal matrix such that $Q\hat{C}^{-1}Q^T =: D$ is diagonal, and defining $R := Q^T\sqrt{D}Q$, we have $R^2 = \hat{C}^{-1}$. Consequently, $\hat{B}^T\hat{C}^{-1}\hat{B} = (R\hat{B})^T R\hat{B}$. The latter matrix represents the scalar products of the entries of $R\hat{B}$. Therefore, if $\hat{B}^T\hat{C}^{-1}\hat{B}$ approaches zero, then $R\hat{B}$ does as well. As no eigenvalue of the positive definite matrix R goes to zero, we conclude that \hat{B} approaches zero.

As a result of this construction, we have $2\hat{B} = A - C + B^T - B$. Since $A - C$ is symmetric and $B^T - B$ is antisymmetric, if their sum approaches zero, then each summand does as well. \square

Lemma 4.2. Suppose the maximal edge length of (Σ, Λ) satisfies $h \leq C^{(8)}$. Then, $\|E_\Lambda\| \leq C_\phi^{(16)}$.

Proof. Let us decompose $\mathbb{R}^{4g} = \mathbb{R}^{2g} \oplus \mathbb{R}^{2g}$ into a black and a white part, and denote the corresponding decompositions of vectors as $P' = P^B \oplus P^W$. By Corollary 3.20, for any such vector P' , we know that $|P'^T E_\Lambda P'| \leq C_{P^B, P^W, \phi}^{(14)}$. Since E_Λ is symmetric, we can find an orthonormal basis of \mathbb{R}^{4g} consisting of

eigenvectors e_i . Let C be the maximum of all $C_{e_i, \phi}^{(14)}$. Then, for all P' with $|P'| \leq 1$, it follows that $|P'^T E_\Lambda P'| \leq C$. Consequently, $|E_\Lambda| \leq \sqrt{2g}C =: C_\phi^{(16)}$. \square

Theorem 4.3. *As the maximal edge lengths of a sequence of ϕ -regular discrete Riemann surfaces on Σ tend to zero, the diagonal blocks of the complete discrete period matrix converge to the same matrix, the off-diagonal blocks converge to the same symmetric matrix, and the sum of a diagonal and an off-diagonal block converges to the period matrix of Σ :*

$$\Pi^{B,W} - \Pi^{W,B}, \Pi^{B,B} - \Pi^{W,W} \rightarrow 0 \quad \text{and} \quad \Pi^{B,W} + \Pi^{B,B}, \Pi^{W,B} + \Pi^{W,W} \rightarrow \Pi_\Sigma \quad \text{as } h \rightarrow 0.$$

In particular, the discrete period matrices converge to their smooth counterpart: $\Pi \rightarrow \Pi_\Sigma$ as $h \rightarrow 0$.

Proof. As $h \rightarrow 0$, the matrix $E_\Lambda^{B=W}$ converges to E_Σ by Theorem 3.19. Let $L := (1_g \quad 1_g)$, and using the representations of E_Σ and E_Λ provided in Lemmas 2.8 and 2.9, as well as the fact that convergence of a matrix to zero in the Frobenius norm implies the convergence of any submatrix to zero, we obtain:

$$L \left(\text{Im } \tilde{\Pi} \right)^{-1} L^T \rightarrow 2 (\text{Im } \Pi_\Sigma)^{-1}, \quad (1)$$

$$L \left(\text{Im } \tilde{\Pi} \right)^{-1} \text{Re } \tilde{\Pi} L^T \rightarrow 2 (\text{Im } \Pi_\Sigma)^{-1} \text{Re } \Pi_\Sigma, \quad (2)$$

$$L \text{Re } \tilde{\Pi} \left(\text{Im } \tilde{\Pi} \right)^{-1} L^T \rightarrow 2 \text{Re } \Pi_\Sigma (\text{Im } \Pi_\Sigma)^{-1}, \quad (3)$$

$$L \text{Re } \tilde{\Pi} \left(\text{Im } \tilde{\Pi} \right)^{-1} \text{Re } \tilde{\Pi} L^T + L \text{Im } \tilde{\Pi} L^T \rightarrow 2 \text{Re } \Pi_\Sigma (\text{Im } \Pi_\Sigma)^{-1} \text{Re } \Pi_\Sigma + 2 \text{Im } \Pi_\Sigma. \quad (4)$$

From the Limits (1), (2), and (3), we deduce the following:

$$\text{Re } \Pi_\Sigma L \left(\text{Im } \tilde{\Pi} \right)^{-1} L^T \text{Re } \Pi_\Sigma \rightarrow 2 \text{Re } \Pi_\Sigma (\text{Im } \Pi_\Sigma)^{-1} \text{Re } \Pi_\Sigma, \quad (5)$$

$$\text{Re } \Pi_\Sigma L \left(\text{Im } \tilde{\Pi} \right)^{-1} \text{Re } \tilde{\Pi} L^T \rightarrow 2 \text{Re } \Pi_\Sigma (\text{Im } \Pi_\Sigma)^{-1} \text{Re } \Pi_\Sigma, \quad (6)$$

$$L \text{Re } \tilde{\Pi} \left(\text{Im } \tilde{\Pi} \right)^{-1} L^T \text{Re } \Pi_\Sigma \rightarrow 2 \text{Re } \Pi_\Sigma (\text{Im } \Pi_\Sigma)^{-1} \text{Re } \Pi_\Sigma. \quad (7)$$

Taking the sum of the Limits (4) and (5) and subtracting (6) and (7), we get:

$$\left(L \text{Re } \tilde{\Pi} - \text{Re } \Pi_\Sigma L \right) \left(\text{Im } \tilde{\Pi} \right)^{-1} \left(L \text{Re } \tilde{\Pi} - \text{Re } \Pi_\Sigma L \right)^T + L \text{Im } \tilde{\Pi} L^T \rightarrow 2 \text{Im } \Pi_\Sigma. \quad (8)$$

The latter can be restated as:

$$\left(L \text{Re } \tilde{\Pi} - \text{Re } \Pi_\Sigma L \right) \left(\text{Im } \tilde{\Pi} \right)^{-1} \left(L \text{Re } \tilde{\Pi} - \text{Re } \Pi_\Sigma L \right)^T + L \text{Im } \tilde{\Pi} L^T - 4 \left(L \left(\text{Im } \tilde{\Pi} \right)^{-1} L^T \right)^{-1} \rightarrow 0 \quad (9)$$

provided that we show

$$2 \left(L \left(\text{Im } \tilde{\Pi} \right)^{-1} L^T \right)^{-1} \rightarrow \text{Im } \Pi_\Sigma. \quad (10)$$

To establish (10), we observe from the Limit (1) that $2\delta := L \left(\text{Im } \tilde{\Pi} \right)^{-1} L^T - 2 (\text{Im } \Pi_\Sigma)^{-1} \rightarrow 0$. We set $T := 1_g - \text{Im } \Pi_\Sigma \left((\text{Im } \Pi_\Sigma)^{-1} + \delta \right)$, which satisfies $|T| = |\text{Im } \Pi_\Sigma \delta| \leq |\text{Im } \Pi_\Sigma| \cdot |\delta| < \frac{\varepsilon}{2|\text{Im } \Pi_\Sigma|} < \frac{1}{2}$, provided that $0 < \varepsilon < |\text{Im } \Pi_\Sigma|$ and h is small enough to ensure $2|\delta| < \varepsilon |\text{Im } \Pi_\Sigma|^{-2}$. In particular, the Neumann

series $\sum_{k=0}^{\infty} T^k$ converges and yields the inverse of $1_g - T = \text{Im } \Pi_{\Sigma} \left((\text{Im } \Pi_{\Sigma})^{-1} + \delta \right)$. Thus,

$$\begin{aligned} \left\| 2 \left(L \left(\text{Im } \tilde{\Pi} \right)^{-1} L^T \right)^{-1} - \text{Im } \Pi_{\Sigma} \right\| &= \left\| \left((\text{Im } \Pi_{\Sigma})^{-1} + \delta \right)^{-1} - \text{Im } \Pi_{\Sigma} \right\| \\ &= \left\| (1_g - T)^{-1} \text{Im } \Pi_{\Sigma} - \text{Im } \Pi_{\Sigma} \right\| = \left\| \sum_{k=1}^{\infty} T^k \text{Im } \Pi_{\Sigma} \right\| \\ &= \left\| T (1_g - T)^{-1} \text{Im } \Pi_{\Sigma} \right\| \leq \frac{\|T\| \cdot \|\text{Im } \Pi_{\Sigma}\|}{1 - \|T\|} < \varepsilon \end{aligned}$$

for any small enough ε . Hence, (10) indeed holds true.

Since $\text{Im } \tilde{\Pi}$ is positive definite by Theorem 2.4, $\left(L \text{Re } \tilde{\Pi} - \text{Re } \Pi_{\Sigma} L \right) \left(\text{Im } \tilde{\Pi} \right)^{-1} \left(L \text{Re } \tilde{\Pi} - \text{Re } \Pi_{\Sigma} L \right)^T$ is positive semidefinite. Also, $L \text{Im } \tilde{\Pi} L^T - 4 \left(L \left(\text{Im } \tilde{\Pi} \right)^{-1} L^T \right)^{-1}$ is positive semidefinite by Lemma 4.1.

We have shown in (9) that the sum of these two positive semidefinite matrices approaches zero. By multiplying with corresponding eigenvectors, we deduce that any eigenvalue of each of the two matrices converges to zero. Since the Frobenius norm is invariant under multiplication with orthogonal matrices, it follows that each individual matrix converges to zero.

Using the boundedness of E_{Λ} by Lemma 4.2, we can apply Lemma 4.1 to deduce that

$$\text{Im } \Pi^{B,W} - \text{Im } \Pi^{W,B} \rightarrow 0 \quad \text{and} \quad \text{Im } \Pi^{B,B} - \text{Im } \Pi^{W,W} \rightarrow 0.$$

From (10), we further deduce that

$$L \text{Im } \tilde{\Pi} L^T \rightarrow 4 \left(L \left(\text{Im } \tilde{\Pi} \right)^{-1} L^T \right)^{-1} \rightarrow 2 \text{Im } \Pi_{\Sigma}, \quad (11)$$

$$\text{so} \quad \text{Im } \Pi^{B,W} + \text{Im } \Pi^{B,B} \quad \text{and} \quad \text{Im } \Pi^{W,B} + \text{Im } \Pi^{W,W} \rightarrow \text{Im } \Pi_{\Sigma}.$$

In analogy to the proof of Lemma 4.1, Limits (7) and (11), together with the boundedness of the positive definite matrix $\text{Im } \tilde{\Pi}$, imply that $\left(L \text{Re } \tilde{\Pi} - \text{Re } \Pi_{\Sigma} L \right) \rightarrow 0$. In particular,

$$\text{Re } \Pi^{B,W} + \text{Re } \Pi^{W,W} \rightarrow \text{Re } \Pi_{\Sigma} \quad \text{and} \quad \text{Re } \Pi^{W,B} + \text{Re } \Pi^{B,B} \rightarrow \text{Re } \Pi_{\Sigma}.$$

Taking the difference, we have $(\text{Re } \Pi^{B,W} - \text{Re } \Pi^{W,B}) + (\text{Re } \Pi^{W,W} - \text{Re } \Pi^{B,B}) \rightarrow 0$. This is the sum of a symmetric and an antisymmetric matrix, so each summand goes to zero. Thus,

$$\text{Re } \Pi^{B,W} - \text{Re } \Pi^{W,B} \rightarrow 0 \quad \text{and} \quad \text{Re } \Pi^{W,W} - \text{Re } \Pi^{B,B} \rightarrow 0. \quad \square$$

In the case of discrete Riemann surfaces based on quad-graphs with orthogonal diagonals, Theorem 4.3 simplifies to the following result:

Corollary 4.4. *For a sequence of ϕ -regular orthodiagonal discrete Riemann surfaces on Σ with maximal edge lengths approaching zero, the blocks of the complete discrete period matrix converge to the real and imaginary parts of the period matrix of Σ :*

$$\Pi^{B,W}, \Pi^{W,B} \rightarrow \text{Im } \Pi_{\Sigma} \quad \text{and} \quad \Pi^{B,B}, \Pi^{W,W} \rightarrow \text{Re } \Pi_{\Sigma} \quad \text{as } h \rightarrow 0.$$

Proof. By Lemma 2.6, $\Pi^{B,W}$ and $\Pi^{W,B}$ are purely imaginary, and $\Pi^{B,B}$ and $\Pi^{W,W}$ are purely real. The convergence result from Theorem 4.3 implies that $\Pi^{B,W}, \Pi^{W,B}$ converge to the imaginary part of Π_{Σ} , and $\Pi^{B,B}, \Pi^{W,W}$ converge to its real part. \square

We aim to deduce the convergence of discrete Abelian integrals of the first kind from Corollary 4.4 and Theorem 3.22, but directly applying Theorem 3.22 to the real and imaginary parts of the multi-valued discrete holomorphic function is not possible since, in general, the black and white b -periods of a discrete holomorphic differential with equal black and white a -periods are not equal.

However, Corollary 4.4 allows us to deduce that these black and white b -periods become equal in the limit. By decomposing $P' \in \mathbb{R}^{4g}$ into its black and white parts as $P' = P^B \oplus P^W$, we can substitute the

matrix $\begin{pmatrix} \operatorname{Im} \Pi_\Sigma & \operatorname{Re} \Pi_\Sigma \\ \operatorname{Re} \Pi_\Sigma & \operatorname{Im} \Pi_\Sigma \end{pmatrix}$, which represents the complete discrete period matrix obtained in the limit,

into the quadratic form E_Λ from Lemma 2.9. With the representation of E_Σ given in Lemma 2.9, we readily verify that $2P'^T E_\Lambda P$ converges to $(P^B)^T E_\Sigma P^B + (P^W)^T E_\Sigma P^W$ as $h \rightarrow 0$.

These two observations imply that in the orthodiagonal case, the discrete Dirichlet energy of the discrete harmonic differential with black periods given by P^B and white periods given by P^W approaches the Dirichlet energy of the harmonic differential with periods given by P , provided the maximum edge length of the ϕ -regular discrete Riemann surface goes to zero and P^B and P^W both converge to P . This property is crucial in the original proof of Theorem 3.22 by Bobenko and Skopenkov [9]. Therefore, employing Corollary 4.4, we can also apply Theorem 3.22 to the sequences of real and imaginary parts of discrete Abelian integrals of the first kind with equal black and white a -periods. This leads us to the following convergence theorem.

Theorem 4.5. *Consider a nondegenerate uniform sequence of orthodiagonal discrete Riemann surfaces (Σ, Λ_n) , where the maximal edge length converges to zero as $n \rightarrow \infty$. Let $\mathcal{A} \in \mathbb{C}^g$ be a given vector of a -periods, and let $(p_n, p'_n) \in E(\Lambda_n)$ be a sequence of edges such that $p_n \rightarrow p \in \Sigma$ as $n \rightarrow \infty$. Denote by Ω the unique holomorphic differential with a -periods given by \mathcal{A} , and denote by ω_n the unique holomorphic differential on the medial graph of Λ_n with equal black and white a -periods given by \mathcal{A} . We normalize the Abelian integral of the first kind $\int \Omega$ to be zero at p , and $\int \omega_n$ is normalized such that $\int \omega_n(p_n) = \int \omega_n(p'_n) = 0$. Then, the discrete Abelian integrals of the first kind $\int \omega_n$ converge to $\int \Omega$ uniformly on each compact subset of $\tilde{\Sigma}$.*

5 Conclusion

The main result of our paper, Theorem 4.3, establishes the convergence of the discrete period matrix to its continuous counterpart for sequences of rather general quadrangulations. We have also specified the limits of the four blocks of the complete discrete period matrix, shedding light on the relation between black and white periods. While in the case of orthodiagonal quadrilaterals, these blocks coincide with the real and imaginary parts of the continuous period matrix, this relation does not hold in the general case, as can be easily verified. Surprisingly, the limit matrix exhibits complete symmetry when black and white periods are interchanged, a notable result considering the general lack of such symmetry at the discrete level. The meaning and implications of this symmetry in the limit, particularly in statistical physics, remain intriguing open questions.

Our proof is conceptually distinct from Bobenko and Skopenkov's approach in [9], despite some similarities. In our proof, neither the black nor the white subgraph plays a specific role, and they can be interchanged. For numerical computations of discrete period matrices of compact polyhedral surfaces, Bobenko and Skopenkov's convergence result [9] and its improved error rate using adapted triangulations [4] are often sufficient, as triangulations are easy to obtain. Quadrangulations, however, offer natural discretizations for *square-tiled surfaces* or *origamis*, which are widely studied translation surfaces [36, 31]. These quadrangulations, consisting of squares, allow for computationally easier parametrizations and subdivisions, enabling precise computation of discrete period matrices for surfaces with not too many vertices. This method was effectively applied by Çelik, Fairchild, and Mandelshtam [12] to approximate the algebraic curve corresponding to a given translation surface. Our Theorem 4.3 not only provides theoretical

confirmation of the convergence observed in [12] on square-lattices but also extends it to quadrangulations consisting of rectangles. This extension allows for a more straightforward approximation of the L-shape with an irrational ratio of side lengths. It also allows for considering affine transformations of square-tiled surfaces, leading to decompositions into parallelograms. The error estimates derived in our proof provide explicit expressions for constants, although in practice, their computation or approximation may be challenging due to their dependence on the derivatives of harmonic functions.

The discrete period matrices corresponding to the L-shaped translational surface obtained by Çelik, Fairchild, and Mandelshtam are exclusively composed of purely imaginary elements. This outcome is expected since the L-shaped translational surface belongs to the class of M-curves, and all discretizations presented in [12] exhibit the same symmetry. Recently, Düntsch's master's thesis [19] delved into this matter. She introduced the concept of discrete real Riemann surfaces and demonstrated that the discrete period matrix of a discrete real Riemann surface shares the same structure as the period matrix of the corresponding real Riemann surface with matching numbers of real ovals and type (dividing or non-dividing). Additionally, she provided characterizations of the complete discrete period matrices of discrete real Riemann surfaces.

However, characterizing the discrete Schottky locus, the space of discrete period matrices of compact discrete Riemann surfaces in the Siegel upper half space, and relating it to the classical Schottky locus remains an open question. Not all discrete Riemann surfaces correspond to polyhedral surfaces [6], prompting us to explore whether the corresponding Schottky loci differ. Further research in this direction may offer new insights into discrete Riemann surfaces and their connections to continuous Riemann surfaces.

Acknowledgment

The author gratefully acknowledges the support from the Deutsche Forschungsgemeinschaft (DFG – German Research Foundation) – Project-ID 195170736 – TRR109. Special thanks to Daniele Agostini, Paul Breiding, Samantha Fairchild, Yelena Mandelshtam, and Türkü Özlüm Çelik for introducing the author to their research on the Schottky problem and demonstrating their interest in employing discrete methods for computing Riemann matrices of translational surfaces. The author also expresses gratitude to Alexander Bobenko and Ulrike Bücking for insightful discussions regarding previous approaches to address the convergence of discrete Riemann surfaces. Moreover, heartfelt thanks go to Günter Rote for resolving the issue of positive semidefiniteness in Lemma 4.1.

References

- [1] D. Agostini, T.Ö. Çelik, and D. Eken. Numerical reconstruction of curves from their Jacobians. In *Proc. of the 18th Conf. on Arithmetic, Geometry, Cryptography, and Coding Theory*, Contemp. Math. AMS, 2021.
- [2] E.D. Belokolos, A.I. Bobenko, V.Z. Enolski, A.R. Its, and V.B. Matveev. *Algebro-geometric approach to nonlinear integrable equations*. Springer Series in Nonlinear Dyn. Springer-Verlag, Berlin, 1994.
- [3] A.I. Bobenko. Introduction to compact Riemann surfaces. In A.I. Bobenko and C. Klein, editors, *Computational approach to Riemann surfaces*, Lecture Notes in Mathematics, pages 3–64. Springer-Verlag, Berlin, 2011.
- [4] A.I. Bobenko and U. Bücking. Convergence of discrete period matrices and discrete holomorphic integrals for ramified coverings of the Riemann sphere. *Math. Phys. Anal. Geom.*, 24:23, 2021.
- [5] A.I. Bobenko and F. Günther. Discrete complex analysis on planar quad-graphs. In A.I. Bobenko, editor, *Advances in Discrete Differential Geometry*, pages 57–132. Springer-Verlag, Berlin, 2016.
- [6] A.I. Bobenko and F. Günther. Discrete Riemann surfaces based on quadrilateral cellular decompositions. *Adv. Math.*, 311:885–932, 2017.

- [7] A.I. Bobenko, C. Mercat, and Yu.B. Suris. Linear and nonlinear theories of discrete analytic functions. Integrable structure and isomonodromic Green's function. *J. Reine Angew. Math.*, 583:117–161, 2005.
- [8] A.I. Bobenko, U. Pinkall, and B. Springborn. Discrete conformal maps and ideal hyperbolic polyhedra. *Geom. Top.*, 19:2155–2215, 2015.
- [9] A.I. Bobenko and M. Skopenkov. Discrete Riemann surfaces: Linear discretization and its convergence. *J. reine angew. Math.*, 720:217–250, 2016.
- [10] D. Braess. *Finite elements: Theory, fast solvers, and applications in solid mechanics*. Cambridge University Press, Cambridge, Third edition, 2007.
- [11] U. Bücking. Approximation of conformal mappings by circle patterns. *Geom. Dedicata*, 137:163–197, 2008.
- [12] T.Ö. Çelik, S. Fairchild, and Y. Mandelshtam. Crossing the transcendental divide: from translation surfaces to algebraic curves. *Exp. Math.*, 34:1–19, 2023.
- [13] D. Chelkak and S. Smirnov. Discrete complex analysis on isoradial graphs. *Adv. Math.*, 228:1590–1630, 2011.
- [14] D. Chelkak and S. Smirnov. Universality in the 2D Ising model and conformal invariance of fermionic observables. *Invent. Math.*, 189(3):515–580, 2012.
- [15] R. Courant, K. Friedrichs, and H. Lewy. Über die partiellen Differentialgleichungen der mathematischen Physik. *Math. Ann.*, 100:32–74, 1928.
- [16] B. Deconinck and M. van Hoeij. Computing riemann matrices of algebraic curves. *Physica D: Nonlinear Phenomena*, 152–153:28–46, 2001.
- [17] R.J. Duffin. Basic properties of discrete analytic functions. *Duke Math. J.*, 23(2):335–363, 1956.
- [18] R.J. Duffin. Potential theory on a rhombic lattice. *J. Comb. Th.*, 5:258–272, 1968.
- [19] J. Düntsch. Real Riemann surfaces – smooth and discrete. Master's thesis, Technische Universität Berlin, July 2023.
- [20] I.A. Dynnikov and S.P. Novikov. Geometry of the triangle equation on two-manifolds. *Moscow Math. J.*, 3(2):419–482, 2003.
- [21] J. Ferrand. Fonctions préharmoniques et fonctions préholomorphes. *Bull. Sci. Math. Sér. 2*, 68:152–180, 1944.
- [22] R.Ph. Isaacs. A finite difference function theory. *Univ. Nac. Tucumán. Rev. A*, 2:177–201, 1941.
- [23] R. Kenyon. Conformal invariance of domino tiling. *Ann. Probab.*, 28(2):759–795, 2002.
- [24] R. Kenyon. The Laplacian and Dirac operators on critical planar graphs. *Invent. math.*, 150:409–439, 2002.
- [25] J. Lelong-Ferrand. *Représentation conforme et transformations à intégrale de Dirichlet bornée*. Gauthier-Villars, Paris, 1955.
- [26] C. Mercat. Discrete period matrices and related topics. arXiv:math-ph/0111043, 2001.
- [27] C. Mercat. Discrete Riemann surfaces and the Ising model. *Commun. Math. Phys.*, 218(1):177–216, 2001.
- [28] C. Mercat. Discrete Riemann surfaces. In *Handbook of Teichmüller theory. Vol. I*, volume 11 of *IRMA Lect. Math. Theor. Phys.*, pages 541–575, Zurich, 2007. Eur. Math. Soc.
- [29] C. Mercat. Discrete complex structure on surfel surfaces. In *Proceedings of the 14th IAPR international conference on Discrete geometry for computer imagery*, DGCI'08, pages 153–164, Berlin, 2008. Springer-Verlag.
- [30] B. Rodin and D. Sullivan. The convergence of circle packings to the Riemann mapping. *J. Diff. Geom.*, 26(2):349–360, 1987.
- [31] G. Shabat. Square-tiled surfaces and curves over number fields. arXiv:2212.07755, 2022.
- [32] M. Skopenkov. The boundary value problem for discrete analytic functions. *Adv. Math.*, 240:61–87, 2013.
- [33] K. Stephenson. *Introduction to circle packing: The theory of discrete analytic functions*. Cambridge University Press, Cambridge, 2005.
- [34] M. Troyanov. Les surfaces Euclidiennes à singularités conique. *Enseign. Math.*, 32:79–94, 1986.
- [35] S.O. Wilson. Conformal cochains. *Trans. Amer. Math. Soc.*, 360(10):5247–5264, 2008.
- [36] A. Zorich. Flat surfaces. In *Frontiers in number theory, physics, and geometry I*, pages 439–585. Springer-Verlag, Berlin, 2006.